INL/EXT-17-43242
Revision 0

Light Water Reactor Sustainability Program

Potential to Extend the Range of Established Online Monitoring Technologies, Such as Guided Waves in Nuclear Power Plant Systems

September 2017

U.S. Department of Energy

Office of Nuclear Energy

INL/ EXT-17-43242
Revision 0

Light Water Reactor Sustainability Program

Potential to Extend the Range of Established Online Monitoring Technologies, Such as Guided Waves, in Nuclear Power Plant Systems

Andrei Gribok

September 2017

Prepared for the
U.S. Department of Energy
Office of Nuclear Energy

Light Water Reactor Sustainability Program

Potential to Extend the Range of Established Online Monitoring Technologies, Such as Guided Waves in Nuclear Power Plant Systems

INL/ EXT-17-43242
Revision 0

September 2017

Approved by:

Name Title [optional]	Date
Name Title [optional]	Date
Name Title [optional]	Date
Name Title [optional]	Date

ABSTRACT

The Light Water Reactor Sustainability Program was initiated to evaluate technologies that could be used to perform online monitoring of piping and other secondary system structural components in commercial NPPs. These online monitoring systems have the potential to identify when a more detailed inspection is needed using real-time measurements, rather than at a pre-determined inspection interval.

This transition to condition-based, risk-informed automated maintenance will contribute to a significant reduction of operations and maintenance costs that account for most nuclear power generation costs.

This report describes the current state of research related to ultrasonic-guided wave testing and its application to defect detection in commercial nuclear power plants. The report analyzes the applicability of the guided wave technology to secondary piping systems, as well as studying the potential for expanding the range of guided wave technology to include bent piping and other piping components. The ultrasonic-guided waves can inspect long stretches of straight piping; however, more complex geometries such as elbows, welds, and tees are causing spurious reflections and coherent noise, which significantly decreases the sensitivity of the technique.

The report also analyzes two approaches to suppress coherent noise in guided wave systems: (1) advanced signal processing and pattern recognition based on independent component analysis, and (2) blind source separation and a hardware-based technique using piezoelectric paint, which can be used to facilitate the propagation of mechanical stress waves through piping. It is demonstrated on simulated guided wave data that the independent component analysis is capable of separating different coherent noise components and segregating them from useful signal. The piezoelectric paint approach seems to be a viable alternative to signal processing methods; however, it requires significantly more complicated logistics and initial financial outlay.

The future efforts will be concentrated on applying the independent component analysis to real-world guided wave data recorded by the guided wave monitoring system installed on the shell of the low-pressure feedwater heater 13A at Exelon Corporation's Braidwood Nuclear Generating Station. Also, the joint EPRI-INL research efforts will focus on experimental evaluation of piezoelectric paint as a technique to extend the range of guided wave technology.

SUMMARY

This report describes the technical potential to extend the range of ultrasonic-guided wave testing in nuclear power plants (NPPs), which is being conducted under the U.S. Department of Energy's (DOE's) Light Water Reactor Sustainability (LWRS) Program.

The LWRS Program, funded by DOE's Office of Nuclear Energy, aims to provide scientific, engineering, and technological foundations for extending the life of operating light water reactors (LWRs). This program involves several goals, one of which is ensuring the safe operation of the passive components in NPPs, such as concrete, piping, steam generators, heat exchangers, and cabling.

Within the LWRS Program, the Advanced Instrumentation, Information, and Control (II&C) Systems Technologies Pathway conducts targeted research and development to address aging and reliability concerns with the legacy analog instrumentation systems, structures, and components (SSCs) and related information systems of the operating U.S. LWR fleet. This work involves two major goals: (1) ensuring legacy analog II&C systems are not life-limiting issues for the LWR fleet, and (2) implementing digital II&C technology in a manner that enables broad innovation and business improvement in the NPP operating model. Resolving long-term operational concerns with II&C systems contributes to long-term sustainability of the LWR fleet, which is vital to the nation's energy and environmental security.

The goals of the LWRS Program are addressed through a number of pilot projects that target realistic opportunities for increasing sustainability, safety, and economic efficiency of the existing NPP fleet. It is generally recognized that the biggest challenge for existing NPPs is economic viability. Reducing operations and management costs are one of the most pressing problems facing the nuclear power generation industry. Operations and maintenance costs comprise approximately 60 to 70% of the overall generating cost in legacy NPPs. Only 15 to 30% of the costs are attributed to obtaining and producing the fuel.

Furthermore, of the operations and maintenance costs in U.S. plants, approximately 80% are labor costs. To address the issue of rising operating costs and economic viability, in 2016, companies that operate the national nuclear energy fleet started the Delivering the Nuclear Promise Initiative, which is a three-year program aimed at maintaining operational focus, increasing value, and improving efficiency.

ACKNOWLEDGEMENTS

The author would like to thank Heather Feldman and Kurt Crytzer of the Electric Power Research Institute (EPRI) for their help and leadership in organizing the joint workshop on structural health monitoring and for providing technical guidance and feedback during the development of the joint research plan. The author is also grateful to Kenneth Thomas of Idaho National Laboratory (INL) for his insights and encouragements during technical discussions.

The authors would also like to extend their special thanks to Alan Puchot of Southwest Research Institute (SwRI) for providing reports, software, and guided wave data. The reports were sources of figures # 10,and 11 used in this report.

CONTENTS

FIGURES

1. ULTRASONIC-GUIDED WAVE TESTING

1.1 Introduction

As a means of defect detection technology, ultrasonic-guided wave (UGW) testing has been successfully implemented in the field of non-destructive examination (NDE) for several years now [1]. The velocity of the guided waves (GWs) is directly dependent on the thickness of the material, which is characterized by the dispersion behavior of the modes of the GWs. Hence, the difference in the thickness of the component will give a variation in the time of arrival of the GW.

Tests conducted by the Imperial College in London have proved the applicability of the utilization of shear horizontal (SH) waves for calculating the average thickness of a plate along a line between two transducers. This work also helped generate a methodology for extracting the value of the thickness measured by SH GW signals, which were characterized by temperature. Application of UGWs to the piping systems of nuclear power plants (NPPs) face additional serious challenges, such as complex geometric shapes, hostile environments, and insulation.

The piping system is one of the most valuable assets in legacy NPPs, with inspections performed on a regular basis. The technical basis for the inspection period could be based on predictive analysis or operating experience, for example. However, because of the significant length of the piping systems, the problem of identifying specific piping components that need to be inspected during an outage remains a challenge. Thus, many unnecessary inspections are performed, which adds to planned downtime and lost revenue. The well-established technology of UGWs offers new possibilities in the inspection of large portions of piping systems with few sensors. UGWs are mechanical or elastic waves that propagate at low frequencies—either sonically or ultrasonically through the walls of a pipe—and bounded and guided by those walls. The velocity and wave modes of GWs are strongly influenced by the geometry of the guiding boundaries. In the pipe, the GWs exist in three different wave modes—longitudinal, torsional, and flexural. Because the GWs are mechanical waves, they are generated either through piezoelectric or magnetostrictive transducers that convert electrical magnetic fields into mechanical energy. Once the mechanical wave is generated with a set of piezoelectric or magnetostrictive sensors arranged in a collar around the pipe, it is transmitted through the walls of the pipe and reflected back from any discontinuities (e.g., flaws) of the surface of the wall, as shown in Figure 1.

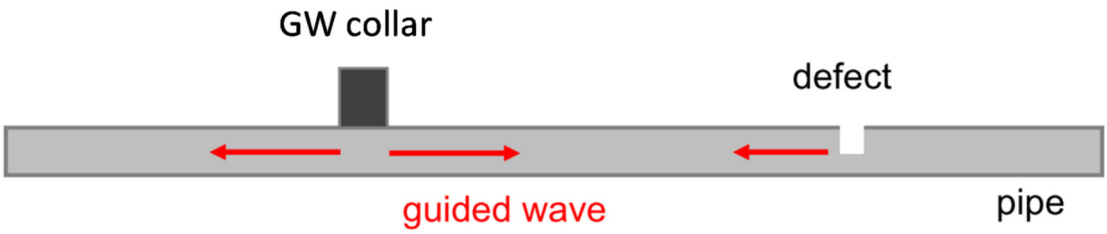

Figure 1. The principle of GW corrosion monitoring (figure source [2]).

GW inspection has numerous advantages over other NDE techniques, including the following:

- It can inspect large sections of piping with a single sweep
- It can inspect inaccessible locations
- Its sensors can be mounted permanently
- It may be used for inspection while the system is operating
- It can inspect pipes from 2 to 96-in. diameter.

The main advantage of GW inspections over conventional ultrasonic testing (UT) inspections is shown in Figure 2. In contrast to conventional UT inspections, the GW technology can cover tens of meters in one inspection session. Traditional UT inspections are highly localized and can only detect flaws within proximity of the sensor location.

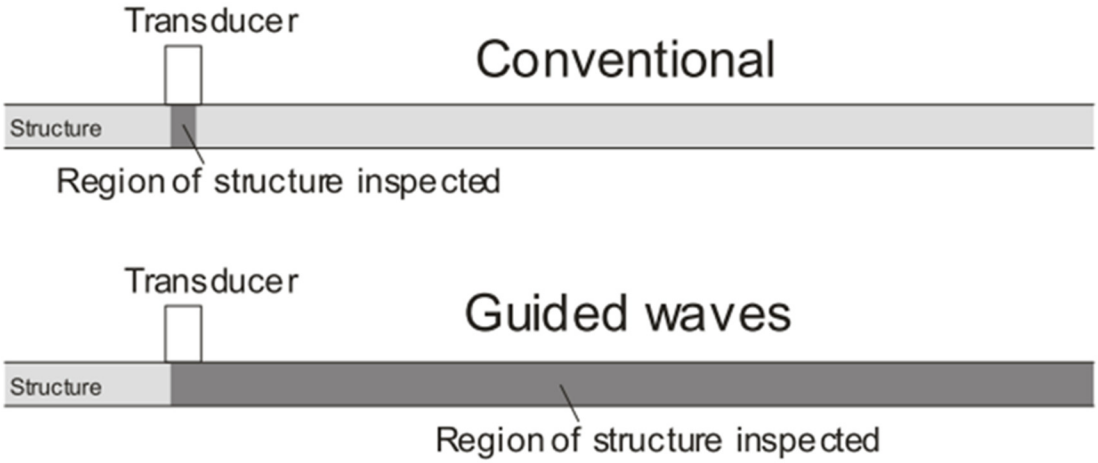

Figure 2. GW inspection versus conventional UT inspection (figure source[2]).

Despite these benefits, GW technology is challenged when applied to power plants in general and NPPs in particular. Piping systems in electric power plants come in various configurations and geometries; for example, they have thousands of elbows, bends, tees, valves, and flanges. These geometries are not a friendly media for GWs. Geometries other than strait pipe attenuate and distort GWs, making inspections beyond them difficult. Also, while being a perfect tool for locating the damage in

pipes, GWs cannot determine the size of the flaw with acceptable accuracy. In summary, provided the GW technology can overcome the limitations of complex geometries, it is a perfect tool for answering the "Where to inspect?" question.

1.2 Physics of Guided Waves

GWs are mechanical stress waves propagating along an object's boundaries and are guided by those boundaries, hence the name. The mechanical stress is generated either through magnetostriction or piezoelectricity. Magnetostrictive materials convert the magnetic field into kinetic energy or stress, while piezoelectric materials convert the electric field into mechanical stress. Both methods have their advantages and disadvantages and are widely used to generate mechanical waves for the purpose of NDE inspection. Both methods generate low-frequency (10-100 kHz) waves with some lying in the audible range to avoid attenuation during propagation though inspected structures. Most methods generate one of three types of GWs: torsional, longitudinal, and flexural modes. These three modes interact with the discontinuities in a pipe and are reflected back to the sensor from those discontinuities, thus pinpointing the location of piping degradation. The longitudinal and torsional waves are most widely used for NDE as the most sensitive to defects. The longitudinal wave is the wave that propagates along the object with compression and rarefication, while the torsional wave is the wave that propagates as results of a medium are being twisted and released.

Ultrasonic methods of fault detection have been effectively used as non-destructive testing (NDT) methods for many years. Conventional UT methods consist of a series of grid tests from the outside surface of the pipe. For consistency, the gridding needs to be the same every time testing is performed. This adds variability to the results and jeopardizes repeatability and reliability of the tests. While being an effective diagnostics tool, this technique has limited coverage; hence, it is time-consuming when insulation covers the pipe, because access to the outside surface requires removal of the insulation each time a test is performed, and further re-installation of the insulation after each test. Moreover, in NPPs, scaffolding is almost always required prior to testing. This adds to maintenance costs and affects the efficiency of the plant. In contrast to conventional UT, UGW testing is a more effective technique for a long-range diagnostic of pipes and metal structures, and has attracted significant attention in recent years. In contrast to regular grid testing, the UGW method largely reduces inspection time and costs for long pipelines. This technique enables pipeline inspections for a long distance from a single position and facilitates defect detection. A UGW collar is installed at one location of a pipe, and reflection echoes indicate the presence of corrosion or other defects. Numerical simulation of GW propagation is an indispensable tool to investigate and understand the behavior of both longitudinal and torsional wave modes. It is also a vital step in the process of development and optimization of nondestructive-testing

procedures based on structural waves. Numerical simulations can often replace physical tests. A 3D model is usually required to simulate wave propagation phenomena with wavelength magnitude when compared to the thickness of the structure.

As stated previously, three possible GWs can propagate along the pipe—longitudinal, torsional, and flexural. Interaction of GWs of different types with geometrical discontinuities and flaws in the structure has been investigated in several works. These studies examined the efficiency of defect detection using longitudinal and torsional modes [3,4,5,6,7]. GWs of the longitudinal mode L(0, 2) are sensitive to defects and are not dispersive. On the other hand, torsional waves T(0, 1) have attractive advantages in defect detection due to their constant speed and propagation when the distance can be estimated as a flight time [8,9,10]. This allows the torsional UGW propagate in a steel pipe. Having a pipe made of homogenic and isotropic material, the problem of guided wave propagation in an elastic isotropic body, which volume K, can be described by the following equations [3, 11]:

$$u = \nabla\phi + \nabla \times \varphi, \tag{1}$$

$$\varepsilon = \frac{1}{2}(\mathrm{grad}(\mathbf{u}) + \mathrm{grad}(\mathbf{u})^T), \tag{2}$$

$$\sigma = \lambda \mathbf{I} \mathrm{grad}(u) + \varepsilon, \tag{3}$$

Where u is displacement, σ is the stress tensor, **c** is the tensor of elastic stiffness, ε is the strain tensor, ρ is the density, u=u(x,t)u=u(x,t) is the displacement vector, and x=(x,y,z)∈Vx=(x,y,z)∈V.

Reformulating in matrix notation, we can write:

$$\mathbf{G}^T(\mathrm{div}) \cdot \mathbf{H} = \rho \ddot{\mathbf{u}}, \mathbf{H} = \mathbf{C} \cdot \mathbf{S}, \mathbf{S} = \mathbf{G}(\mathrm{div}) \cdot \mathbf{u}, \tag{4}$$

where:

$$\mathbf{G}^T(\mathrm{grad}) = \begin{bmatrix} \partial/\partial x & 0 & 0 & \partial/\partial y & 0 & \partial/\partial z \\ 0 & \partial/\partial y & 0 & \partial/\partial x & \partial/\partial z & 0 \\ 0 & 0 & \partial/\partial z & 0 & \partial/\partial y & \partial/\partial x \end{bmatrix}, \mathrm{grad} = \begin{bmatrix} \partial/\partial x \\ \partial/\partial y \\ \partial/\partial z \end{bmatrix}, \tag{5}$$

H=is the stress pseudo-vector, **C** is the matrix of elastic stiffness, and **S**=is the strain pseudo-vector.

In isotropic media, the matrix of elastic constants, $\mathbf{C}$, has the form:

$$C_{11}, C_{22}, C_{33} = \frac{E(1-\nu)}{(1+\nu)(1-2\nu)}, C_{12}, C_{23}, C_{13} = \frac{E\nu}{(1+\nu)(1-\nu)}, C_{44}, C_{55}, C_{66} = \frac{E}{(1+\nu)2}, \tag{6}$$

where E is the Young's modulus and ν is the Poisson's ratio.

We can impose boundary $\mathbf{\Gamma=\partial K}$ of the volume, K.

$$\mathbf{u} = \mathbf{0}, \mathbf{x} \in \Gamma_r. \tag{7}$$

For the end of the pipe, Γ_l, we have:

$$\rho \frac{\partial^2 u}{\partial t^2} = (\lambda + 2\mu) div(divu) + \mu div \times (div \times u), \tag{8}$$

where u is displacment and p=p(x,t) is the pressure vector and λ and μ are Lame constants. For the boundary conditions, $\Gamma_s = \Gamma \setminus (\Gamma_r \cup \Gamma_l)$, is stress free:

$$L^T(\mathbf{n}) \cdot \mathbf{T} = \mathbf{0}, \mathbf{x} \in \Gamma_s. \tag{9}$$

The following initial conditions are introduced:

$$\mathbf{u}(\mathbf{x}, 0) = \mathbf{0}, \mathbf{x} \in V. \tag{10}$$

The problem is solved by finite element method.

Assuming $K_h \subset K$ be the region occupied by the finite element mesh; $K_h = \cup_m \cdot K^{em}$, where K^{em} is a finite element with the number m.

$$\mathbf{u}_h = \mathbf{N}^T(\mathbf{x}) \cdot \mathbf{U}(t), \tag{11}$$

where $\mathbf{N}^T$ are basis functions and $\mathbf{U}$ are displacements.

Using the finite-element technique, approximation can be made related to the basis functions, $\mathbf{N}^T(\mathbf{x})$. Using the above and similar representations for the projection functions for the weak problem statement in K_h, the system of equations could be solved with respect to, $\mathbf{U}$:

$$\mathbf{M} \cdot \ddot{\mathbf{U}} + \mathbf{K} \cdot \mathbf{U} = \mathbf{F}, \tag{12}$$

where $\mathbf{M} = \sum_m^a \mathbf{M}^{em}$, $\mathbf{K} = \sum_m^a \mathbf{K}^{em}$ are matrices, and $\mathbf{F} = \sum_m^a \mathbf{F}^{em}$ is vector of external influences obtained from the element vectors, $\mathbf{F}^{em}$, expressed as:

$$\mathbf{M}^{em} == \int_{V^{em}} (\mathbf{L}(\text{grad}) \cdot (\mathbf{N}^{em})^T)^T \cdot \mathbf{c} \cdot \mathbf{L}(\text{grad}) \cdot (\mathbf{N}^{em})^T dV, \mathbf{F}^{em}, \tag{13}$$

where $\mathbf{N}^{em}$ is the matrix of approximate basis functions, defined for each finite element, and Γ_l^{em} is a boundary that approximates the boundary, Γ_l. The above formulation has been used to obtain simulated torsional GWs to test advanced signal processing techniques.

This model can be used to describe the propagation of both longitudinal and torsional waves. Flexural waves are rarely used in GW systems.

2. APPLICATIONS OF ULTRASONIC-GUIDED WAVES AS AN NDE TECHNIQUE

Preliminary and early prediction of the degradation process in the pipeline systems of NPPs can help prevent catastrophic accidents, such as piping raptures and loss of coolant accidents. Structural health monitoring (SHM) of piping systems is one of the major challenges in current NPP accident scenarios. GW testing techniques are an emerging technology for the NDT of piping systems in power plants. F. Cau et al. [10] conducted preliminary research on the applicability of GW testing to power systems and reached the following results and conclusions:

- Inaccessible pipes can be inspected by implementing a diagnostic system, which is based on neural networks for NDT with ultrasonic waves.
- The finite element method can be deployed for obtaining a desired dataset for training, validation, and testing of signals.
- Feature generation and feature extraction were done so as to make the signals suitable as inputs for neural networks. This was performed by means of fast Fourier transform (FFT) and principal component analysis (PCA) methods.
- The affected region on the pipe probed with a torsional wave became excited by means of a piezoelectric sensor and non-symmetric faults with a variation in the parameters, such as axial position, axial length, angular amplitude, and thickness.
- Under numerical simulation of defects, the preliminary analyzes revealed that the time taken by the reflected signals to reach back to the sensor is proportional to the position of the defect, but independent of the severity of the fault. This idea of time value helps to determine the location of the notch; however, it does not help in determining the degree of degradation.
- It was observed that the classification error distribution of various parameters, such as defect angular amplitude, thickness of the defect, and the axial length of the defect, was accurate. Hence, future research requires the need for developing a signal processing package for the UGW system.

On the other hand, G. Acciani et al. [12] investigated and suggested an automation technique for detecting the sizes of defects caused by corrosion in non-accessible piping systems. Such an approach is characterized by the analysis of the reflection of the ultrasonic echoes by superficial flaws present in the pipes. The reflected signals are processed to obtain a set of reliable features, which are eventually extracted by wavelets transformation, and selection is accomplished by means of a filter method with subsequent optimization through a genetic algorithm. These sets of selected features are then fed into a set of multi-layer perceptron neural networks, which provide the angular and axial dimensions of the flaws. Their conclusions were that applying ultrasound waves yields the following advantages:

- It helps in analyzing long and inaccessible piping systems.
- A significant reduction of human effort via automatic diagnosis.
- It was observed that the classification error distribution of various parameters, such as defect angular amplitude, thickness of the defect, and the axial length of the defect, was accurate. Hence, future research requires the need for developing a signal processing package for the UGW system.

This approach is instrumental in the detection and evaluation of the dimensions of superficial defects in pipes whose shapes do not have a specific dimension. Moreover, this approach is automated, thereby reducing human efforts, and defect dimensions are obtained by using adaptive algorithms obtained from neural networks.

An optical fiber-guided laser ultrasonic system was developed by H. Lee et al. [13] by creating a baseline-free method for the detection of damage for SHM of insulated piping systems under high temperature conditions in NPPs. This method employs an optical fiber with a specially designed lens for focusing, as well as a fixture set up for delivering a Nd:YAG pulse laser to a target excitation point, which is embedded for generating the ultrasonic wave. A second optical fiber is connected between a fiber vibrometer and a point for measurement of ultrasonic wave sensing. The performance of the system was tested at varying temperatures of up to 300°C. Using the axisymmetric behavior of multiple wave propagation paths in pipelines, a baseline-free damage detection algorithm was designed. The baseline-free damage evaluation system has been tested on intact as well as damaged pipe specimens in NPPs.

R. Ahmad and T. Kundu [14] conducted extensive research on a new technique for detecting damage in pipes by propagation of cylindrical GWs through piping systems. They employed continuous wavelet analysis for the identification of defects in pipe networks when the pipes are free in air or a vacuum, as well as when they are buried in the soil. They made the following conclusions:

- Detection of anomalies can be done properly by the right selection of wavelet functions and scaling aspects.

- Efficient study of the integrity of underground piping systems can be achieved by implementing daubechies, symlet, and meyer wavelet functions.

The ultrasonic wave propagation imaging (UWPI) technique [15] investigated the visualization of the damage of pipeline structures by using laser-induced UGWs. The UWPI technique uses a Q-switched Nd:YAG pulsed laser system and a galvanometer-based laser scanner. The dispersion characteristics of the Lamb modes of the pipes were studied where the fundamental frequency was based on the group velocity dispersion curves in the frequency range of 0-500kHz. The A0 mode was dispersive while the S0 mode was constant under 250kHz. The two frequency ranges were separated using digital band-pass filters. The authors investigated the notches and the decrease in thickness for simulation of cracks and erosion, respectively. Irrespective of the shape and geometry of the piping systems, the UWPI images were obtained successfully. Three specific cases were investigated:

- The notch at the site of the welded joint between two straight pipes were examined at ambient temperature conditions.
- The notch on the welded joint between straight and curved pipes were investigated.
- The reduction in the thickness on the curved pipe was also investigated, which showed that the thickness reduction was produced on a specific area while detecting the notch was dependent on a specific time.
- Finally, the notch on welded joints between two straight pipes was examined under high temperature conditions.

Research is currently being carried out for obtaining flaw images with different damage sizes. The angular effect between the damage and the wave front of the forward waves are planned to be studied. These NDT methodologies combined together will be implemented for investigation of composite plates and railway tracks, etc.

GW-focusing techniques for circumferential sizing of defects in piping systems was a subject of recent research [16]. The authors discovered that by means of one circumferential scan of the pipes, multiple locations of defects could be located accurately. If the size of the defects were found to be less than the width of the focal beam, then good circumferential sizing results could be obtained by correlating the experimental reflection profile to the theoretical ones. Circumferential sizing of non-uniform defects and defects having bigger circumferential length could be done from the experimental profile directly. The authors also concluded that the prediction of the results of the sizes of defects are impacted by the shape of the defect, as well as the shape of the angular profile. They suggest that it is better to avoid using angular profiles that have bigger side lobes for better and accurate sizing.

Due to a large number of bent pipes in the piping systems of NPPs, it is extremely important to be able to adapt UGW scanning technology to piping elbows and tees. J. Ni et al. [17] studied various experimental methods to investigate the impact of pipe bend arrangement on GWs-based detection of defects. They conducted research to study the sensitivity of detection at various crack locations using finite element simulations and experiments. The following inferences were drawn:

- Simulation analyzes revealed that the characteristics of GW propagation through the first elbow were not affected by the difference in the configuration of pipe bends.
- At points where the pipes have more than one bend, the energy of the GWs was focused on the extrados of space-Z and plane-Z pipe, but intrados of the U pipe.
- The highest penetration rate was found to be in space-Z pipes when the GWs traverse across it without any defects.
- Along those lines, it was determined that in these pipes the inspection of cracks in the straight pipe beyond two elbows was most sensitive.
- Location of defects and the pipe configurations characterize the sensitivity of detection.

Their study confirmed the possibility of extending the range of UGW over complex geometries.

GWs were also successfully applied for determining the axial length of defects. X. Wang et al. [18] proposed a technique for evaluating the characteristic of axial length defects occurring in pipelines. The basic underlying principle was the consideration that the net reflection produced at the defect is the interference between two primary reflection components, which are the one getting reflected from the front edge of the defect and the other from the back edge of the defect. The axial length under evaluation was found to be directly proportional to the distance between reflection positions at the two edges of the defect. Decomposition and identification of the two reflection signals helps in evaluating the axial length of the defect.

This method has an added advantage as it can be used for investigating more defect parameters and enable comprehensive defect characterization once the two primary edge locations were identified. Respective edge of the defect yields geometric information which can be obtained from the identified edge signal. Employing proper component analysis methods would help in the assessment of radial depth, circumferential extent and other factors of the defect. The results of this research can only be applied to circumferential defects in straight and empty piping systems. However, a generalized implementation of this methods can be deployed in case of real complex situations such as arbitrary shaped localized corrosion defects in different operating circumstances.

Similarly, SH GW testing can be used for estimating the depth of flaws. Estimation and evaluation of the depth of flaws using GW testing with SH GWs is a relatively recent method investigated by A.C. Cobb and J.L. Fisher [19]. The basic principle defining this method is that different wave modes exhibit different particle motions in the direction of the thickness of the material. For the fundamental SH0 mode, the particle motion is constant throughout the thickness, whereas in the SH1 mode, it is higher near the boundaries. The ratio of the response for different modes is used in this approach. The advantage of this technique is that it enables an estimation of depth without using any field portable calibration specimens, which is rare in the case of GW testing. The authors designed a model that could be used for the prediction of the ratio of the amplitude of the signals returning from the flaws. This model has been implemented in plate specimens where a wide range of notch flaws are detected.

In an experiment to test the application and effectiveness of a UGW system, Otero et al. [20] developed two different transducer arrays. The first, seen in Figure 3, is a circular collar containing 14 elements to be placed around a six-inch diameter steel pipe, and the second, seen in Figure 4, is a linear array of 12 elements for use in a steel plate.

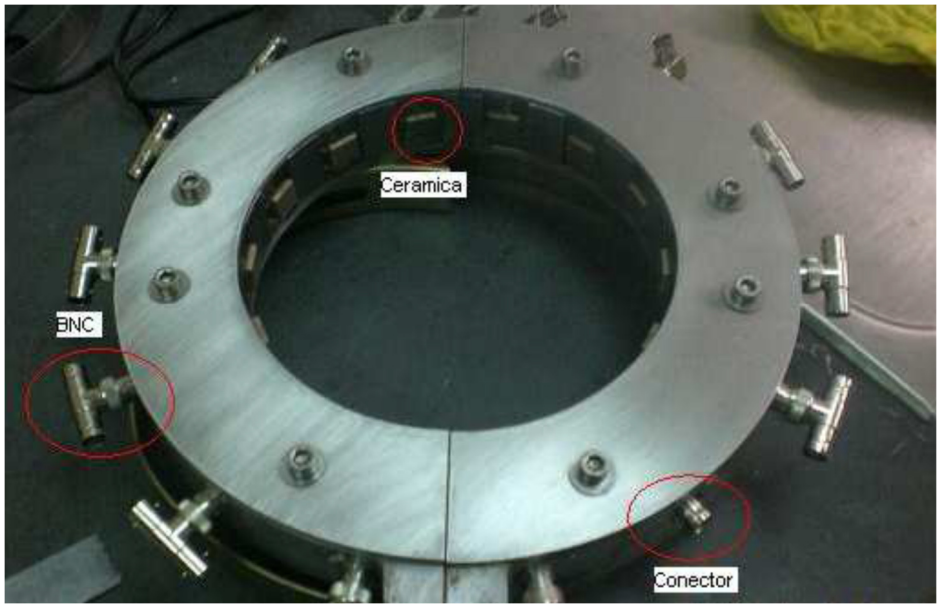

Figure 3. Circular collar transducer array applicable to six-inch diameter steel pipe [20].

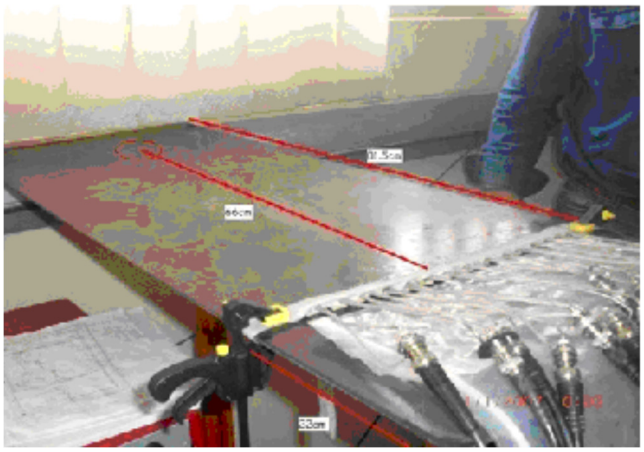

Figure 4. Linear transducer array applicable to steel plate [20].

Experiments on both systems were carried out using a LabView™ interface program, which included the ability to change parameters of the ultrasonic signal, such as frequency, transmitting voltage, and the number of cycles. Other parameters of the system could also be altered independently and included the gain, filter range, and number of channels. Experimental results using both transducers showed that the system was able to effectively detect artificial defects in both the pipe and the plate.

While the use of ultrasonic Guided Wave Testing (GWT) is a highly effective method of detecting corrosion and other defects in long sections of pipe, this method becomes less efficient when dealing with pipe that is either buried in the ground or has been coated/insulated to prevent external corrosion. The range of ultrasonic GWT is significantly reduced in these situations due to the attenuation of the acoustic signal. This is primarily due to two issues: (1) energy-absorbing materials in the waveguide system cause signal dampening; and (2) signal energy travels through the insulation material as well as the section of pipe being tested. The severity of signal loss from both mechanisms are highly influenced by the insulation or coating material.

J.-W. Cheng et al. [21] discovered that a better agreement exists between experiments and predictions for the attenuation of GWs in viscous fluid-filled piping. It was observed that liquid with low viscosity has zero impact on the torsional mode T(0,1), whereas the fluids having higher viscosity that gets deposited in the pipe causes the reflected signal to attenuate by about 25%. Thus, such systems can be implemented in refineries and petrochemical industrial plants for testing of piping systems as a large number of industrial pipelines carry fluids for various manufacturing processes. However, for NPPs, the piping system mostly carries water or steam; as such, attenuation of the ultrasonic signal is minimal.

By applying electromagnetic acoustic transducers (EMATs), M. Gori et al. [22] developed an NDT method that has higher speed and better detecting capability for inspection and monitoring of heat exchangers and boiler tubes. In their research, they designed a rapid non-destructive inspection technique

so as to detect and find the location of the defects in heat exchanger tubes (inner diameter = 10-20mm) and boiler tubes (external diameter = 25-100mm). They used non-contact EMATs that were controlled from a remote position and were operated by SH GWs.

The tube geometry is instrumental in defining the type of probe that can be designed for detecting both transverse and longitudinal waves. This can be achieved by operating the EMATs either from the inner or outer surface. Laboratory tests on heat exchangers and super heater tubes have confirmed that defects having depths up to 1 mm have the ability for localization and remote detection.

Transient acoustic signals have been applied by B. Lu et al [23] for analysis on the structural integrity of a steam generator. The following conclusions came out of their research:

- Lamb waves were used in their study, which were very sensitive towards the structural defects seen in brass tubes. Along those lines, they also observed that defect size, location, shape, and surrounding media in the structure directly impacted the Lamb wave propagation along the guided structures.
- The smallest defect measured was around 1 mm. The smaller microstructural defects could also be monitored easily, as the propagation of elastic waves depend on the microstructure of the materials.
- Four different types of Lamb waves were observed in tubular structures. The Lamb modes are found to be very complex because of the combination of multi-mode waves in plate or tubular structures. Each mode is characterized by a non-linear decrease in speed with an increase in the product of thickness and frequency.
- Hilbert-Huang transform (HHT) was deployed for easy adaptation and separation of sensitive wave modes. This also helps in reduction of unwanted noise in the signals.
- They also used a multi-sensor suite, which comprised two diametrically opposite sensors for separation of single-mode Lamb waves. Anti-symmetric mode signals yielded great results as windows were moved and zoomed towards the signals.
- The increase in the leakage of energy in the Lamb waves was an outcome of submerging the test specimens in water.

The methodologies proposed in this study will be beneficial for online and in-situ monitoring of critical equipment for ensuring safety and reliability of the system as a whole.

Signal attenuation in embedded/burred pipe is critical for extending the range of UGW technology. To determine the amount of attenuation of the signal in embedded pipe, Leinov et al. [24,25] conducted an experiment to determine the different factors that affect the attenuation of the signal in terms of the embedded material. A 5.67 m long, 8 in. diameter carbon steel pipe was used as the test specimen, 3m of

which was embedded in a specifically designed container to simulate the embedded section of the pipe. A drawing of the apparatus can be seen in Figure 5(a) and 5(b).

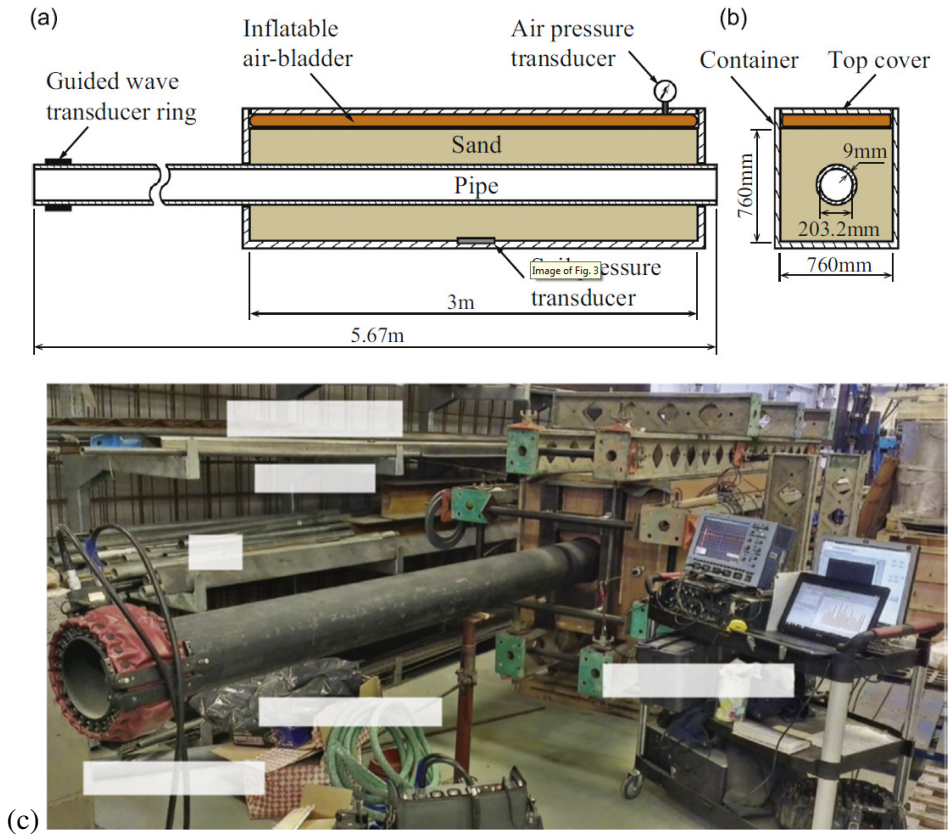

Figure 5. Experimental apparatus: (a) side view, (b) front view, and (c) general view [25].

This experiment used five different embedded material characteristics: dry loose sand, dry compacted sand, dry mechanically compacted sand, water saturated sand, and drained sand. An inflatable air-bladder was also used to apply pressure on the section of pipe to simulate several different depths of the buried pipe. The experiment concluded that increased pressure and compaction of the sand resulted in an increase in the attenuation of the signal; therefore, it can be assumed that an increase of buried depth and compacted material will cause a significant decrease in the applicable range of ultrasonic GWT.

In a different but very similar experiment using the same experimental apparatus, Leinov et al. [25,26] attempted to determine the effect of a fusion-bonded epoxy (FBE) coating on a similarly sized section of pipe under similar conditions. The thin coating of FBE was determined to slightly increase the amount of attenuation in comparison to the previous study. Due to the increased benefits of the coating in terms of external corrosion, ultrasonic isolation of the section of pipe was then demonstrated using a Polyethylene (PE)-foam layer between the coated pipe and the sand. Due to the PE-foam layer having a smaller impedance than both the pipe and the sand, a reduction in the leakage of the ultrasonic signal into

the surrounding sand resulted. Without this isolation, it was estimated that propagation distances on the coated pipe were approximately 10 m, while isolating the pipe using the PE-foam increased this distance to approximately 15-30 m. Thus, the FBE can be used as an efficient technique to extend the range of the UGW technique.

In another similar experiment, but on a much smaller scale, Ahmad [26] attempted to determine propagation effects of a buried pipe with active flow. Typically, when a section of pipe needs to be inspected, the pipe is excavated and the coating is removed, if present. Also important to note is that the flow of the pipe is typically shut down prior to any testing. Both procedures are time-consuming. The described experiment was aimed at discovering what effects this active flow had on GW propagation. It was discovered that the overall strength of the signal in a pipe with active flow is reduced compared to that with no flow. However, on several occasions enhanced propagation was observed and proved to help in the identification of defects.

Study of signal attenuation plays an important role in UGW testing. In a paper aimed to explain methods, application, and current research being conducted in the field of GWT, Lowe & Cawley [27] discuss the mechanisms that cause signal attenuation in GWT. They noted the following:

- Attenuation due to the type of material, including any coating present.
- Scattering caused by a rough surface produced by corrosion.
- Reflections from features in the pipe, such as welds or supports.
- Mode conversion of the signal caused by bends, which causes a reduction in applicable range.
- Leakage in instances of embedded pipe.

These same authors go on to discuss how bends in a pipe can affect the applicability of GWT, as most systems will contain bends. Authors state that typical pulled bends in a pipe do not present a high level of difficulty in assessing test readouts for defects using GWT. The problem arises when the pipe contains sharp bends created by two sections of pipe welded to an elbow. The bend causes a mode conversion of the signal, which requires a technician with a high skill level in order to differentiate between the reflected signal of the welds surrounding the bend and the defects present in the pipe. They also note that while it is possible to test sections of pipe with multiple bends, it is recommended to limit testing to sections containing only one bend and to place the bend at the far end of the test range in order to alleviate complications of interpreting the reflected signal.

One of the main problems when testing sections of pipe using UGW is the fact that signals are not only reflected from the defects present, but also from welds and other features of the pipe. In a paper

discussing the application of UGW, Cawley [28] describes a method to eliminate this misinterpretation. He suggests that by using an axially symmetric mode when utilizing UGW, any reflected signals from uniform welds or flanges will only reflect an axially symmetric mode. In a vast majority of cases, corrosion defects will not form in a uniform fashion and only reflect non-axially symmetric signals. The graphs in Figure 6(a) and 6(b) represent this difference.

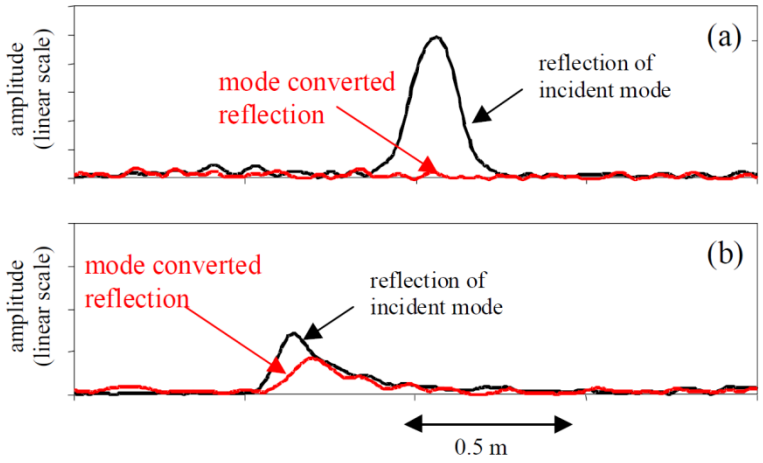

Figure 6. (a) Uniform feature (weld), (b) corrosion [28].

As can be seen in Figure 6, the mode-converted reflection of the uniform weld does not reflect a non-axially symmetric mode, while in the case of corrosion it does. This is a fairly basic concept to avoid—the common misinterpretation of welds in a pipe as corrosion—especially when sections of the pipe are not visible, as well as to significantly increase the range of UGW testing.

In a study aimed to provide an overview of the wide range of applications for UGW, Rose [29] provided details on two prominent concepts of utilizing UGW to inspect pipes. These concepts are axisymmetric inspection and focused pipe inspection. In an axisymmetric inspection, the individual sensors within the collar, similar to that in Figure 3, are pulsed in phase to produce an axisymmetric wave that uniformly moves along the pipe. In a focused pipe inspection, a focused beam revolves around the circumference and down the pipe using a prescribed time delay profile. Graphical representations of the axisymmetric and focused pipe inspection concepts can be seen in Figures 7 and 8, respectively.

Figure 7. Axisymmetric GW inspection displaying wave propagation at specific times along the length of a pipe [29].

Figure 8. Focused GW inspection displaying focused beam at specific times as it moves around and along the length of pipe [29].

Also in this study, the author provided detailed lists of the accomplishments and obstacles of using UGW to inspect pipes. Some mentioned successes in the field include:

- Knowledge of axisymmetric and non-axisymmetric modes.
- Great penetration power with the use of specialized sensors is produced.
- Defect size detection to less than 5% of cross-sectional area (CSA).
- Location and length of defect estimations with focusing.
- Ability to test pipes with insulation or coatings.

Obstacles to using this method include:

- Inspections on sections of pipe with numerous tees, elbows, bends, and the ability to inspect beyond an elbow are limited.
- Pipes with active fluid flow cannot be scanned.
- Reliability and difficulty in correctly identifying defects compared to other pipe features, such as welds.
- Ability to reliably detect defects beyond the first major defect is limited.

Due to its ability to scan long stretches of straight piping, the UGW is most applicable for use in the crude oil pipeline industry. In an experiment to study the relationship between received signal parameters and pipe wall integrity, Mokhles et al. [30] performed UGW testing on sections of a crude oil pipeline. Most of the pipeline system had not been used in over 40 years. However, the sections that were recently replaced provided a healthy comparison between the old and new sections of the piping system. Out of a total of 527 possible locations, only 35—25 from the old pipe and 10 from the new pipe—were selected for testing for comparison purposes. In each test location, pipe wall thickness was measured in four locations around the circumference of the pipe. In the new sections of pipe, the variance between these four measurements is relatively low due to the lack of internal corrosion, whereas the variance in the sections of old pipe were much higher due to the presence of corrosion. This is called the variance factor and was used as the basis of comparison to the signal parameters in those specific locations. In order to obtain an enhanced comparison, the signal/noise ratio was divided into the attenuation value for each location results, which is referred to as the comparison factor. A graph of this relationship can be seen in Figure 9.

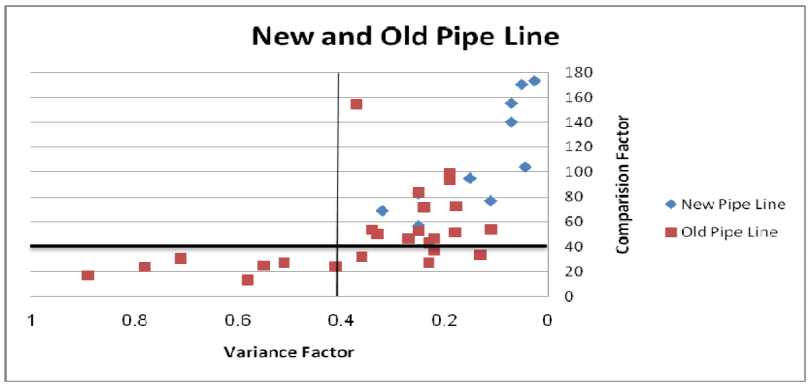

Figure 9. Relationship between variance factor and comparison factor in 35 test locations of crude oil piping [30].

As can be seen in Figure 9, all of the points for the new pipe have a low variance factor and a relatively high comparison factor due to the lack of corrosion. It was determined that anything with a variance factor greater than 0.4, and a comparison factor less than 40, should be considered a high-risk location. The use of this relationship is a much faster approach than other methods as it allows for a quick analysis of long sections of pipe to determine the areas that pose the greatest risk.

W.-B. Na and T. Kundu [31] studied the applicability of UGW to underwater piping systems and reached the following conclusions:

- A new advanced coupler mechanism was developed so as to study the plausibility of flexural cylindrical GWs for detecting defects in underwater piping systems.
- GWs were generated, propagated, and received with the assistance of incident angle adjustment and frequency sweep techniques. The new coupler method and GWs proved to be an efficient device and an effective tool for SHM of underwater piping systems.
- Analytical study of the dispersion curves of aluminum surrounded by water showed the presence of a number of modes. It was observed that the flexural GW modes closer to the asymptotes of the dispersion curves have a higher sensitivity than those that are far away from the asymptotes.

This research proved that the new transducer holder and its coupling mechanism can be used for underwater pipeline monitoring by using UGWs.

In a technical review, P. Rizzo [32] made an extensive study on various NDE methods for SHM on water and wastewater piping systems. He suggests the following NDE techniques for inspecting water mains and wastewater piping networks:

- Electromagnetic methods:
    - Eddy current
    - Ground-penetrating radar
    - Magnetic flux leakage.
- Mechanical methods:
    - Acoustic emission
    - Ultrasonic testing
    - Impact echo method
    - Acoustic leak detection
    - Sonar.

- Visual inspection methods:
    - Closed-circuit television (CCTV) examination.

Surface anomalies in wastewater pipes inspected by means of CCTV, laser-scanning, or sonar could be improved by enhancing the resolution of images obtained from the CCTVs. The author proposed that a trenchless untethered system that can probe the structures from inside without disrupting service can be highly beneficial. The SHM techniques for pipelines also comprise various other important issues, such as modelling of damage, establishing criteria, and the process for setting up indices for evaluation of damage or defects.

In another study about the detection of pipe wall damage, M. Vasiljevic et al. [33] proposed the use of GWs generated by an EMAT system. Cylindrical GWs having longitudinal modes L(0,1) and L(0,2) were created and discovered in a metal pipe by means of EMATs. The authors analysed the signal both before and after multiple propagations of different wave modes inside the pipe, which helped in overcoming the problems associated with the identification of the small signal from the defect and the truncation of the signal after the defect signal, but much prior to the arrival of the reflected signal from the end of the pipe.

The signal could be stabilized by multiple reflections and scattering of the traversing wave modes by the pipe ends and the defects that help in generating consistent spectral plots. These plots provide substantial evidence for differentiation of defective pipe and defect-free piping systems. For the precise prediction of the location of the defect, the signal must be identified in time history plots.

Application of UGW technology to piping requires sophisticated signal processing and pattern recognition techniques, as well. R. Ahmad and T. Kundu [34] investigated the performance of various signal processing methodologies in GW applications for detection of defects in pipeline networks. They analyzed the following techniques and approaches:

- FFT of experimental signals provides information regarding the modes of propagation; thus, it also helps in identification of the modes that are more sensitive to defects.
- Comparison of different wavelet coefficients for pipes under various boundary conditions helped in finding the defective pipes via continuous wavelet analysis methods.
- Mother wavelet functions might be used for differentiating a defective pipe from a defect-free pipe.

A. Demma et al. [35] performed a comparative study to investigate the effects of defect size on the reflection of GWs in piping systems. They presented the following parameters:

- Maps that denote the reflection coefficient as a function of depth and circumferential extent of the defect.

- A T(0,1) incident was discovered at 35 kHz.
- A correction factor for different pipe sizes was estimated.
- Location of the defect in the cross-section.
- Ultrasonic GW mode was used.
- Frequency of excitation.

Practical testing knowledge helped in getting information regarding the circumferential extent of the defect from mode conversion by means of the Flexural/Axisymmetric (F/A) ratio.

An estimation of the defect could be easily made by implementing maps defining the minimum and maximum reflection coefficient denoted as a function of circumferential extent and depth of defect. The maximum reflection coefficient map is used in the case of a wide frequency range, whereas the minimum reflection coefficient map is used in the case of a narrow frequency bandwidth.

In their experiments on GW-based pipe inspection, P. Sun et al. [36] proposed a new EMAT system to evaluate stainless steel heat exchanger tubes in the shell of a heat exchanger. They further improved the structure of the EMAT and worked on suppressing the unwanted mode formed during the experiment. The EMATs for GW inspection of pipes are generally placed on the outer surface of the pipes. But in the case of heat exchangers, most of the area within consists of the space enclosed by the shell and the tube surfaces, thus not allowing outer surface placement of the transducers. Existing methods involve inserting a probe into the heat exchanger tube from one end in order to inspect the tubes. Specially-developed EMATs have long been used to generate and receive torsional waves, but these are again affected by the plates supporting the tubes.

Recently, using GWs in order to inspect heat exchanger tubes has gained particular interest as the transducer need not be pulled across the length of the entire tubing for inspection. Rather, both contact and non-contact GW sensors are used. This method has a very high efficiency defect detection rate and is of primary importance when the number of tubes to be inspected is very large. EMATs are used to produce GWs in the heat exchanger tubes using electromagnetic coupling without any requirement of physical contact with the tubes.

EMATs based on Lorentz force were used to inspect stainless steel pipes with weak magnetostrictive force. Torsional waves were excited by the Lorentz force within the heat exchanger tube. These waves are essential in detecting both circumferential and longitudinal cracks. In their work, P. Sun et al. [36] developed an EMAT to evaluate heat exchanger tubes made of stainless steel with the assistance of the L(0,2) mode, which can be operated at higher frequencies and is non-dispersive. This EMAT works on the principle of radial and axial non-uniform static magnetic fields.

The conclusions of the work described in their paper can be summarised as follows:

- Unlike conventional EMATs, the new design works with static magnetic fields consisting of both axial and radial components.
- Experimental and simulation results suggest that the EMAT can transmit and receive L(0,2) mode GWs.
- An unwanted L(0,1) mode is also received in the signal, which has to be suppressed. Mode control is achieved by using two repelling permanent magnets at a spacing of L, within the receiver structure.
- With the improved transmitter and receiver structures, mode control is achieved and the amplitude of the unwanted L(0,1) mode is significantly reduced.
- This kind of mode control only works in the longitudinal +Z direction and not for –Z direction. For the latter, damping substances need to be used at the other end in order to reduce the effect of elastic waves.

Mode conversion is also seen in the case of non-axially symmetric defects.

K. Sinding et al. [37] described a successful and effective means of utilizing NDE and SHM techniques for steam generators where ultrasonic transducers having the ability of withstanding high temperatures can be implemented. This approach also demands a stronger coupling of the transducers to the complex geometries of the heat exchangers at elevated temperatures. Their purpose was to make use of piezo electrics in the deposition of comb transducers to the curved surface topography.

They concluded that the spray-on transducer deposition method enabled them to have a better strength in coupling of composite transducers to the pipe substrates. It was observed that the PZT/Bismuth Titanate were able to transmit and receive the second harmonic waves. They also have the capacity to withstand thermal ratcheting at high temperatures of about 400°C. They also plan to perform these tests with Bismuth Titanate and Lithium Niobate composite material.

Dispersion analysis of multi-layered structures is described by M. Bezdek et al. [38] where they used two different modelling techniques; hence ,they made the following inferences:

- The matrix methods theory with special attention given to multi-layered waveguides having liquid layers was used.
- A numerical approach for generating dispersion curves, which were characterized by the matrix methods, were used.

- The finite-element method (FEM) approach was implemented for the simulation of the waveguide set-up inclusive of real-world wedge transducers.
- They also used a 2-D model of the setup and a post-processing technique for procuring group velocity dispersion diagrams.
- The verification and validation of the model was done by using theoretical and experimental results.
- Furthermore, the authors introduced sample dispersion diagrams for a couple of various other wedge angles, α; thus, eventually they were compared to the modal solutions of the matrix methods. Finally, these FEM simulation results were used for the depiction of displacement profiles across the waveguide.

H. Kwun et al. [39] conducted detailed research regarding bore testing of heat exchanger tubing using a long-range GW probe in torsional mode. The probe design comprises a hollow cylinder waveguide, which is attached with a magnetostrictive sensor. This sensor assists in the generation and detection of torsional waves in the waveguide. Experimental set up consisted of the waveguide, which was inserted at one end of the tube, and the tip of the waveguide, which was expanded to make close contact with the inner surface of the tube. This results in mechanical coupling of the torsional waves from the waveguide to the tube and vice versa. Data were obtained from tubes made of different materials like ferrous and non-ferrous tubes and different geometry like U-bend tubes and finned tube, etc. The long-range testing plausibility of the probe was studied. Field evaluation, verification, validation, and robustness of the probe has ensured an enhanced performance. It can be used in industry soon.

Implementation of circumferential GW for the detection of crack has been a topic of interest to material scientists. Y.-M. Cheong et al. [40] conducted research using a technique for studying axial crack in feeder piping systems. A circumferential GW technique was applied for detecting axial cracks on the bent parts of the feeder pipe. Dispersion curves generated from circumferential GWs were calculated as a function of the curvature. For infinite curvature (i.e., in case of thin plates) with an increase in frequency, the S_0 and A_0 coincide eventually with the Rayleigh wave mode. However, in the case of pipes, with an increase in curvature, even at higher frequencies the lowest modes do not coincide. After reviewing the acoustic velocity and dispersion curves, it was found that the surface waves propagating along the inner and outer surface were ultrasonic waves generated by the rocking technique. The authors observed that it is ideal to use long-range axial GW techniques for general investigation of the pipe, whereas circumferential GW techniques should be used for quantitative analysis of the location and size of the defects. They also inferred that the application of circumferential GW techniques for investigating a feeder pipe was limited for the following reasons:

- High-radiation exposure for the ultrasonic experts who examine the pipe.
- Less accessibility to the bent region.

3. ANALYSIS OF MSS DATA COLLECTED ON THE BRAIDWOOD HEAT EXCHANGER SHELL 13A

Southwest Research Institute® (SwRI®) developed a proprietary GW-based corrosion monitoring system utilizing magnetostrictive sensor (MsS) technology developed and patented by SwRI to monitor corrosion in large secondary structures of NPPs [41]. The description of the MsS system provided in this section and results, follows descriptions presented in [41]. In October 2010, the system's prototype was installed on the shell of low-pressure feedwater heater (FWH)13A at Exelon Corporation's Braidwood Nuclear Generating Station. The system generates UGWs of different modes that can propagate over large areas in metal cylinders to screen a structure for damage.

SwRI partnered with Exelon to install the system on FWH13A. A total of 17 magnetostrictive sensors were installed on the heat exchanger shell in a layout designed to provide maximum monitoring coverage over the surface of the shell. The monitoring system was activated in testing mode in January 2011 and collected guided-wave monitoring data on the shell until the following July. At that time, SwRI discontinued the collection and reviewed the data for preliminary analysis. As pointed out in [41,] "SwRI was able to identify several features in the GW baseline waveforms (inspection mode review) that corresponded to areas of wall-thinning identified in October 2007 by standard gridded ultrasonic inspection, which was performed by Exelon". Some of the other features identified in the ultrasonic inspection data were not detectable in the GW data due in part to the positioning of the MsS probes with respect to the undetected features [41]. After initial inspection, SwRI concluded that maximizing the monitoring coverage over the shell is not as important as providing sufficient coverage in key regions.

After initial testing, the system collected GW data for 747 days between January 27, 2011 and February 12, 2013.

Having analyzed the data, SwRI identified five sensors located around the January 27, 2011, to February 12, 2013, for the 17 MsS probes installed on the heater shell. SwRI performed periodic review and analysis of the data from the probes located near the East and West inlet nozzles for evidence of corrosion activity. Over the two-year period, SwRI identified a total of 17 locations of corrosive activity around the East inlet nozzle and 14 locations around the West inlet nozzle.

The main data analysis tool applied by SwRI to evaluate six months of collected data (e.g., through July 2011) was the normalization and subtraction of the newly collected data from the baseline data (monitoring mode review) to look for changes and degradation progression in the shell condition with

time. As of July 2011, no definitive evidence of corrosion degradation was observed. The minor acoustical response indicates only minor corrosion degradation on the shell, but at the detected amplitudes, it is difficult to estimate the magnitude of the detected degradation.

Analyzing the data, two inlet nozzles at the top of the shell has been determined that showed good potential for detecting future changes in the shell condition. Based on the preliminary success of the MsS monitoring system, Exelon contracted SwRI to provide ongoing analysis of the data collected by these five sensors [41]. While SwRI analyzed only five sensors, Idaho National Laboratory (INL) intends to analyze all 17 sensors using advanced signal processing and pattern recognition techniques.

The MsS monitoring system installed on FWH13A consists of one MsSR3030 unit, an MsS Multiplexer, a control computer, and 17 MsS plate probes. A conceptual block diagram of the system is shown in Figure 10.

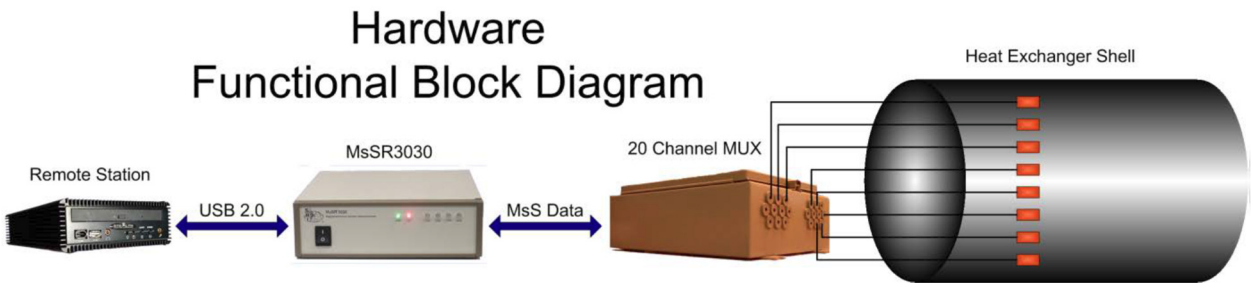

Figure 10. MsS monitoring system hardware block diagram (figure source[41]).

As reported in [41], "the control computer includes a software module that regulates the data sampling and organizes and stores the collected data by acoustical sensors. The software provides interfaces to retrieve the data either through an Ethernet connection or radio communication to a local network." The data are recorded in proprietary format and require a Matlab code to convert them into ASCII. Due to safety regulations, at the time of installation, the system was not connected to the plant network. Instead, all data were recorded and a software function was added to automatically upload all collected data onto an external USB drive when a drive is detected on the front panel USB port [41].

Over a period of more than two years, SwRI has reviewed the data collected by five previously identified MsS probes (e.g., S4, S5, S6, S18, and S19) installed on the Braidwood Generating Station low pressure FWH13A for analysis. The location of the probes and the shell thickness as measured by ultrasonic gridding method are shown in Figure 11. The monitoring system detected a total of 17 indications of possible corrosion near the East inlet nozzle (component AIR13-FAC-80) and 14 indications of possible corrosion near the West inlet nozzle (component AIR13-FAC-78) [41].

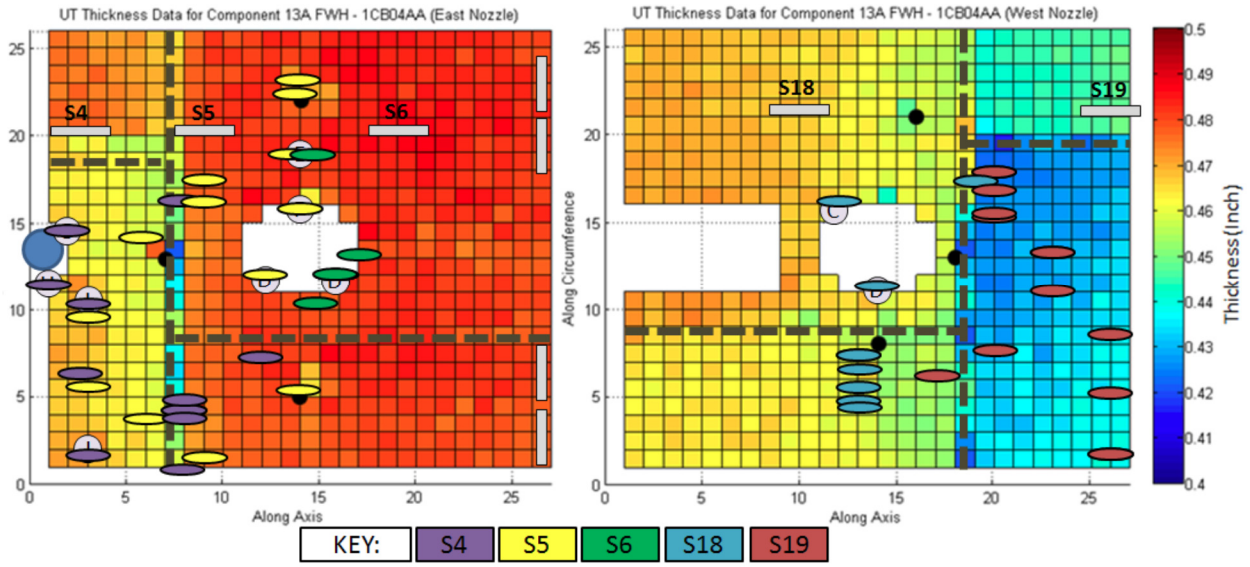

Figure 11. Probes placement around the East (left) and West (right) inlet nozzle over the monitoring period. The locations of the probes are superimposed over the gridded ultrasonic thickness measurements taken during periodic maintenance in October 2017, (figure source[41]). .

According to [41], following data revision and analysis, it was found that all the repeatable and recordable corrosive degradation appeared in the upper part of the heater shell within the gridded regions surrounding the two inlet nozzles. These regions are shown in Fig. 11. Also "the greatest concentration of corrosive degradation occurred around the two inlet nozzles, shown in Fig. 11, near the circumferential welds within the gridded regions and within the thinner plates of the shell that were located just beyond the circumferential welds". As reported in [41], "Evidence of corrosion degradation was noted on both pits to the North and South of the East inlet nozzle and on the pit to the North of the West inlet nozzle, but indications of change within these regions did not appear until nearly the end of the monitoring period" [41].

According to [41,] "throughout monitoring, none of the reflected signals exceeded 21 mV in differential signal amplitude, indicating that the shell experienced only a very minor change in wall thickness over the monitoring period". As was expected, although the MsS technology appears to have the capability of locating corrosion activity in a heat exchanger shell, it is difficult to estimate the magnitude of corrosion activity. The relatively low signal amplitudes and data complications encountered during analysis make magnitude estimation unreliable. INL's contribution to this technology consists in developing advanced signal-processing and pattern-recognition techniques that allow detecting small thickness degradations and estimating the degree of degradation [41].

4. APPLICATIONS OF INDEPENDENT COMPONENT ANALYSIS TO SIMULATED GUIDED WAVES SIGNALS

As was emphasized in previous sections, for UGW to be a competitive technology in the nuclear industry, it needs to overcome several shortcomings, such as low sensitivity to minor degradation, dependence on piping geometry, and a low signal-to-noise ratio in a heavily degraded piping environment. This report aims to address the low signal-to-noise ratio by applying advanced signal processing techniques capable of dealing with coherent noise, which is endemic in UGW systems.

The reflected signals recorded with UGW systems usually consist of several peaks that correspond to reflections from different features of the structure under inspection, such as welds, supports, elbows, or areas of corrosion and erosion. In addition to these peaks, there is background noise that mainly happens due to the following reasons:

- the material will usually exhibit low-level surface roughness that is caused by the interaction of the ultrasonic signal with the structure
- ultrasonic mode conversions.

When the ultrasound interacts with a feature, coating, or surface roughness, some of the energy will be converted into different wave modes. If a mode is dispersive, it will contribute to the background signal (noise) as it spreads out in time and space.

Ideally, a UGW technique will only transmit the non-dispersive wave modes; however, interaction of the ultrasonic wave modes with non-axisymmetric features of the pipe can lead to mode conversions. This results in the generation of dispersive wave modes (DWM). To increase the defect sensitivity and improving the signal-to-noise ratio of reflection from features, it is important to filter out the DWM as much as possible. The background noise produced by dispersion is coherent (non-random) and overlaps in frequency domain with the signal of interest. Since the DWM is non-random, it cannot be tackled through averaging or other noise-reducing techniques. Conventional techniques, such as using low-pass and high pass filters or averaging, became unable to reduce the background noise. Independent component analysis (ICA) or blind source separation is a technique that can deal with non-random coherent noise. This technique uses knowledge of the dispersion characteristics of the wave mode, such as non-Gaussianity deconvolve signals in the time domain. It does not rely on frequency characteristics, but rather on statistical properties of signal and noise. This technique is rooted in a traditional statistical method—PCA—and extends it to the independent signals, while traditional PCA can only tackle uncorrelated signals. In the case of Gaussian-random variables, independence and lack of correlation are equivalent, which is why the assumption of non Gaussianity becomes critical for this technique. However,

in the case of UGW testing, this assumption is perfectly legitimate since the reflected waves are periodic signals with non-Gaussian distributions.

4.1 Principal Component Analysis

The basic PCA approach linearly transforms a data matrix of p columns (sensors) and n rows (observations) to an orthogonal principal components space of equivalent dimensions [42]. The transformation occurs such that the direction of the first principal component is determined to capture the maximum variation of the original data set. The variance of subsequent principal components is the maximum available in an orthogonal direction to all previously determined principal components. The full set of principal components is an exact copy of the original data set, though the axes have been rotated. Selecting a reduced subset of components results in a reduced dimension structure with the majority of the information available, in which information is assumed to be equivalent to variance. Usually, small variance components that are not retained are assumed to contain unrelated information such as process or measurement noise.

In the context of redundant instrument channel monitoring, it is assumed that the first principal component can provide an estimate of the true measured parameter, and the smaller variance components are assumed to be negligible with respect to the estimation. To avoid ambiguities in the terminology, the set of orthogonal components derived from PCA, which are sometimes referred to as principal component scores, will be referred to herein as principal components and denoted in matrix form as Z. The transformation of the data matrix to the principal component matrix is given by:

$$\mathbf{Z} = \mathbf{XA} \tag{14}$$

where $\mathbf{Z}$ is the $(n \times p)$ principal component matrix, $\mathbf{X}$ is the $(n \times p)$ matrix of *mean-centered* measurement data with n observations, and p redundant sensors. $\mathbf{A}$ is the $(p \times p)$ matrix of eigenvectors of $\mathbf{X}^{\mathbf{T}}\mathbf{X}$. The following notation is also defined as:

- $\mathbf{a_j}$ is the j th eigenvector of $\mathbf{X}^{\mathbf{T}}\mathbf{X}$, where $j = 1,..., p$, of dimensions $(p \times 1)$
- $\mathbf{z_j}$ is the j th principal component, where $j = 1,..., p$, of dimensions $(n \times 1)$
- $z_{i,j}$ is the scalar value of the j th principal component corresponding to the i th
- (i =1,...,n) redundant measurement vector $x_{[i,:]}=[x_{i,1}, x_{i,2}, \ldots x_{i,p}]$.

Due to the commonly valid assumption that a set of redundant instrument channel measurements can be approximated by the first, or primary, principal component; an estimate of the *mean-centered* true value of the process at the i th sample is given by:

$$p_i = z_{i,j} = x_{[i,:]} a_1. \quad (15)$$

For the full data matrix **X**, we can write:

$$p = z_1 = X a_1, \quad (16)$$

where p_i is a scalar *mean-centered* estimate based on $x_{[i,:]}$, **p** is a vector *mean-centered* estimate based on **X**, of dimensions ($n \times 1$).

Finally, we define the parameter estimate after mean-centered scaling, in scalar and vector form, as:

$$p_i^f = p_i + m_x^w, \quad (17)$$

$$p^f = p + \begin{bmatrix} 1 \\ 1 \\ \vdots \\ 1_n \end{bmatrix} \cdot m_X^w, \quad (18)$$

where

$$m_X^w = \left[a_1^T \cdot \begin{bmatrix} \bar{x}_{[:,1]} \\ \bar{x}_{[:,2]} \\ \vdots \\ \bar{x}_{[:,p]} \end{bmatrix} \right] \cdot \frac{1}{\sum_{j=1}^{p} a_{j1}}, \text{ (the eigenvector weighted mean value)}, \quad (19)$$

$$\bar{x}_{[:,p]} = \frac{1}{n} \sum_{i=1}^{n} x_{[i,p]} \text{ (the mean value of the } p \text{ th channel)}. \quad (20)$$

Obviously, if the channels are identical, the first principal component will be an equal combination of each channel, if and only if:

$$\bar{x}_{[:,1]} = \bar{x}_{[:,2]} = \cdots = \bar{x}_{[:,p]}, then\ a_{11} = a_{12} = \cdots = a_{p1} = \sqrt{\frac{1}{p}}. \quad (21)$$

In general terms, if an input channel's variance is higher than the remaining channels, its corresponding element in the eigenvector of the first principal component will also be higher. Thus, the influence of a particular channel's measurements on the final parameter estimate can be related to that channel's sample variance. In an on-line monitoring approach, a set of measurement data would be used to calculate the eigenvector, **a**, the mean values of the redundant channels, and the weighted mean value, *m*. Subsequent estimations could then be produced based on future observations via:

$$p_k^f = x_{[k,:]} a_1 + m_x^w, \quad (22)$$

where $x_{[k,:]}$ is the vector of future observations and p_k^f is the corresponding estimate.

In applying the PCA method for GWs signal processing, it is important to keep in mind the theoretical assumptions that support such an application. It is assumed that the first principal component contains enough information about the parameter of interest, and that the variance of the concurrent channel measurement vectors is related to the overall process in such a way that higher variance

measurements should be allowed a greater influence on the parameter estimate. Due to the underlying importance of the sample variance calculations for this method, it should be verified that the data being used are free of outliers. The residuals between the resultant parameter estimate, shown in equation 22, and each redundant channel measurement are then evaluated for each observation in an on-line mode, or alternatively in a batch mode. Sensors are considered resolved when a channel's residual deviates from some nominal value determined during the calculation of the model parameters using a representative data set.

The PCA is usually performed on test data from pipe loops that have been subject to multiple temperature cycles both in undamaged and damaged states, such as introduced defects and corrosion. In addition to processing data from experimentally controlled damaged conditions, simulated damage signals are added to "undamaged" experimental data, so enabling multiple different damage scenarios to be investigated. The algorithm has also been used to process GW signals from finite element simulations of a pipe with distributed shallow general corrosion, within which there is a patch of severe corrosion.

4.2 Independent Component Analysis and Blind Source Separation

ICA was introduced in the early 1980s and attained wide attention and growing interest in the mid-1990s. The technique attempts to identify original signals from a mixture of observed signals, which are a linear combination of sources, without knowing any information about the mixing matrix, or having any prior information about the sources except that they are assumed to be independent and have non-Gaussian distributions.

Since the sources are assumed to be independent they are termed independent components (ICs). One requirement for isolation of the ICs is that only one component can have a Gaussian distribution. A detailed survey of ICA can be found in *Neural Computing Surveys* [44] and also in [43,45]. ICA is rooted in the need of finding a suitable linear representation of a random variable. The classic method to solve this problem is to use second order information in the covariance matrix, such as principal component analysis and factor analysis [42]. Rather than applying independence as a guiding principle, PCA attempts to linearly transform a data set resulting in uncorrelated variables with minimal loss of information [45]. For Gaussian-distributed variables, uncorrelatedness is identical to independence. For non-Gaussian-distributed variables, independence is a much stronger requirement than uncorrelatedness.

For non-Gaussian data, higher-order statistics are needed to obtain a meaningful representation. Projection pursuit is a technique for finding interesting features of data such as clusters using higher order statistics [46]. Projection pursuit uses a cost function such as differential entropy [46] rather than the mean-squared error used in the PCA transformation. Projection pursuit is effective for the non-Gaussian

data sets. There are similarities and connections between ICA and these techniques. In the noise-free case, ICA is a special case of projection pursuit. ICA can also be viewed as a non-Gaussian factor analysis. ICA must use higher order statistics while PCA only uses second order statistics.

However, ICA is still not a mature technique and remains in the development process. Many practical problems beyond the basic ICA model exist. Some include the nonlinear mixing problem [47], underdetermined ICA model (i.e, more sources than sensors [48]), noisy ICA [49], and the nonstationary problem [50]. For a nonstationary signal, alternative assumptions other than non-Gaussianity of ICs are needed. One can use different autocovariance functions [51] or nonstationary variances [50] for a successful separation.

The user should be very cautious at the application of statistical learning methods by fully understanding the basic underlying assumptions for any applications. This is also true for sensor validation using ICA. In the next section, the method of classic ICA is discussed. For the task of UGW signal filtering, a prior information of non Gaussianity is used to identify a proper IC. Moreover, a unity check is derived for ICA reliability monitoring.

4.3 Information Theory Background

The ICA model can be understood more easily from the viewpoint of information theory [52]. The concept of entropy is the basis of the information theory. For a given random variable, X, with probability density, p(x), the entropy, H(X), is defined by Shannon [53]:

$$H(x) = -\sum p(x) \cdot \log(p(x)) = E\left[\log(\frac{1}{p(x)})\right], \tag{23}$$

where E(·) denotes the expectation operator. Entropy gives a measure of randomness for the given distribution. The measure of entropy for a rare event will be large, so a large amount of information is due to this event. For a continuous variable, the differential entropy is introduced by changing the summation to an integral [54]. Consider a discrete histogram:

$$H = -\lim_{N_B \to \infty} \sum_{i=1}^{N_B} p(x_i)\, \Delta \log(p(x_i)\Delta), \tag{24}$$

taking the limit, we obtain:

$$H = -\int p(x) \log\big(p(x)\big)\, dx + \lim_{N_B \to \infty} \log(\Delta). \tag{25}$$

Omitting the constant, differential entropy of a continuous random variable is:

$$H = -\int p(x) \log\big(p(x)\big)\, dx. \tag{26}$$

For two distribution p(x) and q(x), the Kullback-Leibler entropy [52] is a measure of the difference between the two distributions and defined as:

$$H(p,q) = -\sum p(x) \cdot \log\left(\frac{p(x)}{q(x)}\right). \quad (27)$$

Notion of entropy was initially introduced by C. Shannon in 1949. His primary goal was to find a measure of "randomness" of a discrete probability distribution. According to Shannon [53]: "Suppose we have a set of possible events whose probabilities of occurrence are p_1, p_2,…,p_n. These probabilities are known but that is all we know concerning which event will occur. Can we find a measure of how much 'choice' is involved in the selection of the event or of how uncertain we are of the outcome?

If there is such a measure, say $H(p_1,p_2,\ldots,p_n)$ it is reasonable to require of it the following properties:

1. H should be continuous in p_i.
2. If all p_i are equal $p_i = 1/n$, then H should be a monotonic function of n. With equally likely events there is more choice, or uncertainty, when there are more possible events.
3. If a choice is broken down into two successive choices, the original H should be a weighted sum of the individual values of H. That is, for example H(1/2,1/3,1/6)=H(1/2,1/2)+1/2*H(2/3,1/3)."

Shannon [53] points out that the only H satisfying the three assumptions above is of the form:

$$H = \sum_{i=1}^{n} p_i \cdot log\frac{1}{p_i} = -\sum_{i=1}^{n} p_i \cdot logp_i, \quad (28)$$

with the convention for $p_i = 0$ 0*log1/0 = 0 since. If the base of log is 2 entropy measured in bits, if 10 in digits, if e in nits. Shannon called the value $-\log p_i$ a piece of information or "surprise." For example, if p_i approaches 0, then we will be very surprised to see the i – th event and the formula says $-\log(p_i)$ approaches ∞. On the other hand, if $p_i = 1$, then we won't be surprised at all to see the i – th event and the formula says $-\log(p_i) = 0$. Looking at the formula for entropy, we see that it is the average over "surprise" which in its turn depends explicitly on p. The entropy thus can be viewed as a "self-moment" of the probability, in contrast to ordinary moments; for example, $E(x^2)$, which are averages over quantities that do not depend on p. The entropy and other self-moments contain a very different kind of information than the ordinary moments. Entropy measures the average degree of surprise that one should feel upon learning the results of measurements with probability distribution $p_1,p_2,\ \ p_n$. Shannon's entropy for discrete random variables, possesses the following useful properties:

1. Entropy reaches its max when $p_1 = p_2 = \ldots = p_n$.
2. $H \geq 0$ with equality iff $p_i = 0$ for one i.
3. Entropy is additive for independent variables:

H(x,y)=H(x)+H(y) iff P(x,y)=p(x)p(y).

4. The conditional entropy of x given y:

$$H(x/y) = \sum\sum p(x,y)\log\frac{1}{p(x/y)} \quad , \tag{29}$$

this measures the average uncertainty that remains about x when y is known.

5. Joint entropy:

$$H(x,y) = \sum\sum p(x,y)\log\frac{1}{p(x,y)} . \tag{30}$$

6. The mutual information between x and y is:

$$I(x,y) = H(x) - H(x/y) , \tag{31}$$

or

$$I(x,y) = H(x) + H(y) - H(x,y) , \tag{32}$$

because knowing y cannot make x more uncertain H(x) ≥ H(x/y) and hence I(x,y)≥0. I(x,y)=I(y,x).

Information measures the average reduction in uncertainty about x that results from learning the value of or vice versa. Equivalently, it measures the amount of information that x conveys about y. Mutual information is a measure of statistical dependence. Two random variables have zero mutual information if and only if they are statistically independent. This can be seen from the following inequality:

$$I(x,y) = \sum\sum p(x,y)\log(\frac{p(x,y)}{p(x)p(y)}) \geq \sum\sum p(x,y)(1-\frac{p(x)p(y)}{p(x,y)}) \geq \sum\sum p(x,y) - \sum\sum p(x)p(y) = 0 \tag{33}$$

We have used the fact that log(x)≥1-1/x. Equality hold only if x=1, hence only when p(x,y)=p(x)*p(y).

To estimate mutual information between random variables, we need to estimate probability density function of random variables x and y, and joint probability function of x and y. The estimate of marginal pdf's is one dimensional histogram, where $p_i = N_i/N$ for a given binsize Δx. The estimate of joint probability function is bi – dimensional histogram, where $p_{i,j} = N_i/N$ for binsize ΔxΔy. In the multidimensional case, the mutual information is called "redundancy:"

$$R(x_1, x_2, ...x_n) = \sum_{i=1}^{n} H(x_i) - H(x_1, x_2, ...x_n) . \tag{34}$$

R is the number of bits that are redundant in *a* vector measurements. The redundancy occurs because the knowledge of some components of *a* vector measurements can be used to predict something about other components. It can be shown that for Gaussian variables redundancy can be defined as:

$$L(x_1, x_2, ...x_n) = -\frac{1}{2}\sum_{i=1}^{n}\log\sigma_i , \tag{35}$$

where σ_i are eigenvalues of the correlation matrix. L is called linear redundancy. Sometimes it is helpful to have normalized redundancy, which is called predictability:

$$PR = \frac{R(x_1, x_2, ...x_n)}{\sum_{i=1}^{n} H(x_i)}, \tag{36}$$

and linear predictability:

$$LPR = \frac{L(x_1, x_2, ...x_n)}{\sum_{i=1}^{n} H(x_i)}. \tag{37}$$

4.4 Practical Implementation of Independent Component Analysis and Blind Source Separation

ICA is a statistical framework in which the observed data, X, are expressed as a linear transformation of latent variables ('ICs', S) that are non-Gaussian and mutually independent. We may express the IC model as:

$$X = A\ S, \tag{38}$$

where X is an (n x p) data matrix of n observations from p sensors, S is an (p x n) matrix of p ICs, and A is an (n x p) matrix of unknown constants, called the mixing matrix.

The problem is to determine a constant (weight) matrix, **W,** so that the linear transformation of the observed variables:

$$Y = W\ X, \tag{39}$$

has some suitable properties. In the ICA method, the basic goal in determining the transformation is to find a representation in which the transformed components, *yi*, are as statistically independent from each other as possible.

When random variables with specific non-Gaussian distributions are combined, the central limit theorem shows that the sum is more Gaussian than the original variables. Therefore, to separate the original variables (S) from a sum (X), we want to choose a transformation (W) that makes them as non-Gaussian as possible. We then assume that the maximally non-Gaussian signals, Y, are estimates of the original ICs, one of which is the parameter value, and thus the parameter estimate.

Hyvarinen [43] developed an ICA algorithm called FastICA as described below. It uses negentropy J(y) as the measurement of the non-Gaussianity of the components:

$$J(y)=H(y_{Gauss})-H(y), \tag{40}$$

where H(y) is the differential entropy of a random vector *y*,

$$H(y) = -\int f(y)\log\big(f(y)\big)\,dy, \tag{41}$$

where f(y) is probability density function of random vector y.

Based on the maximum entropy principle, negentropy J(y) can be estimated:

$$J(y_i) \approx c[E\{G(y_i)\} - E\{G(v)\}]^2, \tag{42}$$

where G is any nonquadratic function, c is an irrelevant constant, ν is a Gaussian variable of zero mean and unit variance, and E{ } is the operator of mathematical expectation.

One attempts to maximize negentropy so that a non-linear transformation of y is as far as possible from a nonlinear transformation of a Gaussian variable (v). This nonlinear transformation (G) is also called a contrast function. The following is a commonly used contrast function, G, and its derivative, g:

$$G(u) = \frac{1}{a_1}\cdot logcosh(a_1 u), g(u) = \tanh(a_1 u). \tag{43}$$

The FastICA algorithm for estimating several ICs is described below:

1. Center the data to make its mean zero.
2. Whiten the data to give **z** with unit variance.
3. Choose *m*, the number of ICs to estimate.
4. Choose initial values for the **w**i, *i*=1,…,m, each of unit norm. Orthogonalize the matrix **W** as in step 6 below.
5. For every *i*=1,…,m, let $w_i \leftarrow E\big[z\{G(w_i^T z)\} - E\{g(w_i^T z)\}\big]^2 w$ (44)

where G and g are defined in:

5. Perform a symmetric orthogonalization of the matrix $\mathbf{W=(w1,\ldots,wm)^T}$ by $\mathbf{W}\leftarrow (\mathbf{WW^T})^{-1/2}\mathbf{W}$.
6. If matrix has not converged, go to step 5.

A concern while using ICA is that it has two ambiguities [45]. One is that the variances (energies) of the ICs cannot be determined. The other is that the order of the ICs cannot be determined. These ambiguities are of concern when performing on-line instrument channel monitoring for two reasons: (1) the components must be scaled back to their original units, and (2) the component containing the parameter estimate needs to be selected.

To scale the components back to their original units, we need to calculate the correct scale factor, α, by selecting the component corresponding to the parameter of interest. To do this, the mean of the measured parameter is estimated by taking the mean of the medians for each (*i*) of n channels (see

equation 38). Next, compute n scale factors by dividing the mean of the parameter by the mean of each component and use those scale factors to give the components the same mean as the measured parameter. The scaled component with the highest correlation coefficient to the raw signals (X) is the component of interest and is the parameter estimate:

$$\alpha_i = \frac{mean(median(X))}{median(IC_i)}, i = 1, \dots, n, \tag{44}$$

where X is the matrix of n mixed signals ICi is the ith IC. To calculate the correct transformation matrix, rescale the transformation matrix **W** to **Wc**: Wc = sign (α) * α * W, where α is the αi that maximizes the correlation between the scaled component and the parameter value. The parameter estimate is now calculated with:

$$\mathrm{Y} = \mathbf{W_c}\,\mathrm{X}. \tag{45}$$

As stated by many authors, and validated by our own research, many ICA methods are shown to work satisfactorily in computer simulations, but perform poorly in real environments. One reason is the actual signals found in practice are commonly nonstationary. For these cases, other separation principles should be used. Since U.S. NPP signals are usually stationary, the ICA algorithm is used in conjunction with a simple method to detect any nonstationary conditions called a unity check.

For the model,

$$y = \sum_{i=1}^{n} w_i x_i. \tag{46}$$

Taking the expectation of both sides of equation 46 results in:

$$E(y) = \sum_{i=1}^{n} w_i E(x_i) \tag{47}$$

Since *xi* are redundant sensor measurements and is the parameter estimation, the expectations would give the same value resulting in:

$$\sum_{i=1}^{n} w_i = 1 \tag{48}$$

Since there are uncertainties in the estimation, a tolerance check is used:

$$\left| \sum_{i=1}^{n} w_i \right| - 1 < \varepsilon \tag{49}$$

where ε is a measure of uncertainty. For ε = 0.05, there is 10% uncertainty in the estimation.

The unity check uses *a priori* information. It is used to determine whether the ICA algorithm is operating correctly and indicates when it fails: such as when the signals are nonstationary. If ICA fails to

pass the unity check, direct averaging is used for parameter estimation. This results in the ICA algorithm being used when the signal is stationary and direct averaging being used during transients.

4.5 Performance of ICA on Simulated Guided Wave Signals

Applying UGW technology, it is possible to inspect long stretches of straight pipelines from a single location; a single collar of sensors can routinely inspect up to 100 m of pipe [55] under ideal conditions. However, such long coverage is a compromise between length of inspection and sensitivity to changes in cross-section with most UGW systems capable of resolving up to 5% of wall thickness change [56]. This is the reason for combining UGW with gridded ultrasonic inspections in NPPs [41]. The GW has full volumetric coverage and propagates well in steel, making it especially suited for long-range screening applications without many bent pipes.

A number of commercially available UGW systems is available all operating using a collar of ultrasonic sensors attached to the outside of the pipe or other metal structure, such as the heat exchanger shell [57,58,59]. The collar emits a magnetic or electrical pulse, which is converted into a mechanical stress wave, which propagates along the pipe. Once the guided stress wave reaches a place with different impedance, part of it is scattered back and received by the same sensor using inverse magnetostriction or piezoelectricity. Often, the impedance change reflects the change in wall thickness due to corrosion of other degradation mechanisms. However, the impedance is also changed at other piping structures such as bents and supports. Due to this spurious reflection, an experienced operator is required to interpret the scattering results to make a decision about the level of degradation [60,61]. In addition to these spurious reflections, there are also unwanted modes and noise from the control system [62,63]. All this additional signals create background noise that significantly reduces the signal-to-noise ratio, which should be at least two for the genuine defects to be detected. However, the major problem with background noise in UGW systems is not its magnitude but its deterministic nature, such noise is known as coherent noise and it cannot be removed through traditional filtering techniques due to the overlap in frequency domain with useful reflections [63]. While there are standards for collecting and interpreting the GW data, their applications require an experienced and trained operator. Introducing an operator into the measurement chain, however, creates an additional problem of interpretability and repeatability of the results. Initially, the UGW systems were used as an inspection device without permanently mounting the system on the inspected structure, one the measurement is collected the device is moved to a different location and the other set of measurements will be collected. Recently, more and more UGW systems are installed permanently due to a couple of reasons: (1) cost of installation, which includes removing insulation and scaffolding, and (2) improved defect detection and classification using baseline subtraction technique. The high access cost is especially strong motivation for permanently installed sensors in NPPs. It is a

well-known fact that in the nuclear industry, the cost of NDT logistics is higher than the cost of NDT per se. The other driver is high repeatability and reliability of the sensor readings due to the exclusion of human error from the measurements. Once the system is permanently installed, its initial readings can be used as a baseline measurement and all subsequent measurements will be compared against it by subtracting the baseline from them. This baseline subtraction will effectively remove the coherent noise and improve system's sensitivity for fault detection. However, the baseline subtraction is only effective if the changes are due to structural degradation of the structure, if the changes are due to ambient conditions of the pipe such as temperature or pressure, the baseline subtraction will not work since the baseline itself has changed [64]. One way to tackle the problem is to collect several baselines under different operating conditions and use the most appropriate baseline to compare to future readings [64], this however is not feasible in power systems due to a large number of operating conditions. To address this shortcoming, an improved technique, called "baseline stretching" has been developed that attempts to compensate for baseline change due to temperature by stretching or dilating the baseline depending on the conditions. This way, the technique compensates for the difference in propagation velocity due to temperature [65]. The approach is not fool proof, however, as the stretching does not compensate the difference in the baseline accurately and the performance of the method deteriorates significantly when the temperature difference in increasing. This is the reason behind research on baseline-free compensation and denoising techniques [65,66,67]. Such established statistical techniques as PCA, Singular Value Decomposition (SVD), neural networks, and support vector machines (SVM) were applied to UGW data collected under different environmental conditions. In these studies, these techniques were able to compensate for environmental and operational changes and extract a representation of the defect with lower coherent noise than the original signal; in other words, the signal-to-noise ratio was above one. ICA is similar to PCA and SVD in that it transforms the data to extract meaningful representation. All these techniques are unsupervised in that no operator input is required to tell signal from noise.

The difference between ICA is that the linear techniques use a decorrelation of the data to separate the sources, while ICA minimizes the mutual information between independent sources. The purpose of this report is to investigate the potential of ICA for processing the signals obtained through simulation of GWs propagation in pipes. This is accomplished by applying ICA to signals recorded in real-world of monitoring conditions that we might deal in the industry.

The intention of using ICA on GW data is that after applying the transform, one of the ICs will contain data relating to the defect, while most coherent noise will be rejected to other ICs; thereby giving a clearer representation of the defect. Numerous implementations of ICA are available, but the FastICA algorithm [43] is used in this study because it achieves similar performance to other algorithms but at

greater speed. As described in Section 4.4, FastICA is formulated as a linear model in Eq. (38). When applied to the analysis of the GW signals, X in (38) will be the [nxp] data matrix of GW signals or mixtures from p sensors each containing n time samples that can be converted to distance knowing the wave's velocity. S is a matrix of ICs representing the signals reflected from defects and coherent noise. The expectation is that the defect signal and coherent noise are statistically independent, which is a valid assumption since they are produced by independent sources. FastICA performs minimization of mutual information or negentropy to obtain demixing matrix W and apply it to the original signals X:

$$S = WX. \tag{50}$$

To obtain W, FastICA iterates through different values of W while, maximizing the independence of columns in matrix S.

When applied to GW data, the rows of source matrix, S, will be GW signals containing the reflections from different features, while the columns of A show the amplitude of these signals across the input data. The columns of A, therefore, track the amplitude values of the rows of S, the ICs. In this report, all columns of A are divided by the maximum value in that column, so the max value becomes one, with the amplitude of the rows of S also adjusted. Multiplying rows of S and weighting function W we can obtain the signal's amplitude. The amplitude between A and S is invariant and can be adjusted. The next step is to undercover defect growth information in rows of S. When the defect location is known, we can select the source that is most similar to the defect reflection response. However, to apply the method in practice with unknown defects and their locations, it will be necessary to produce an automatic method to distinguish components relating to true defect growth from those relating to random noise or environmental effects. A number of methods have been proposed in the literature [69], but so far it has only been proven on step-type defect growth. One potential alternative is change detection using the generalized likelihood ratio, as reported in [70].

We applied models (13) and (38) to generate sources shown in Figure 12. The original sources represent simulated reflections obtained using models (13) and (38). From top to bottom in Figure 12, the reflections are: defect reflection, weld reflection, temperature effect reflection, and random noise.

The mixed signals are shown in Figure 13. These are the signals registered in matrix X and they represent the signals arriving to the sensors location. The assumption is that there are four sensors. The results of application of standard signal processing algorithms, such as PCA, are shown in Figure 14. We can see that while the PCA was able to segregate the weld reflection, it is unable to reconstruct other independent sources thus failing to achieve independences between signals. Figure 15 shows results of applying FastICA to the mixtures. We can see a dramatic difference with results in Figure 14 as all

independent sources are separated and are similar to the ones shown in Figure 12. Notice that signal separation can only be achieved up to the ordering of the components.

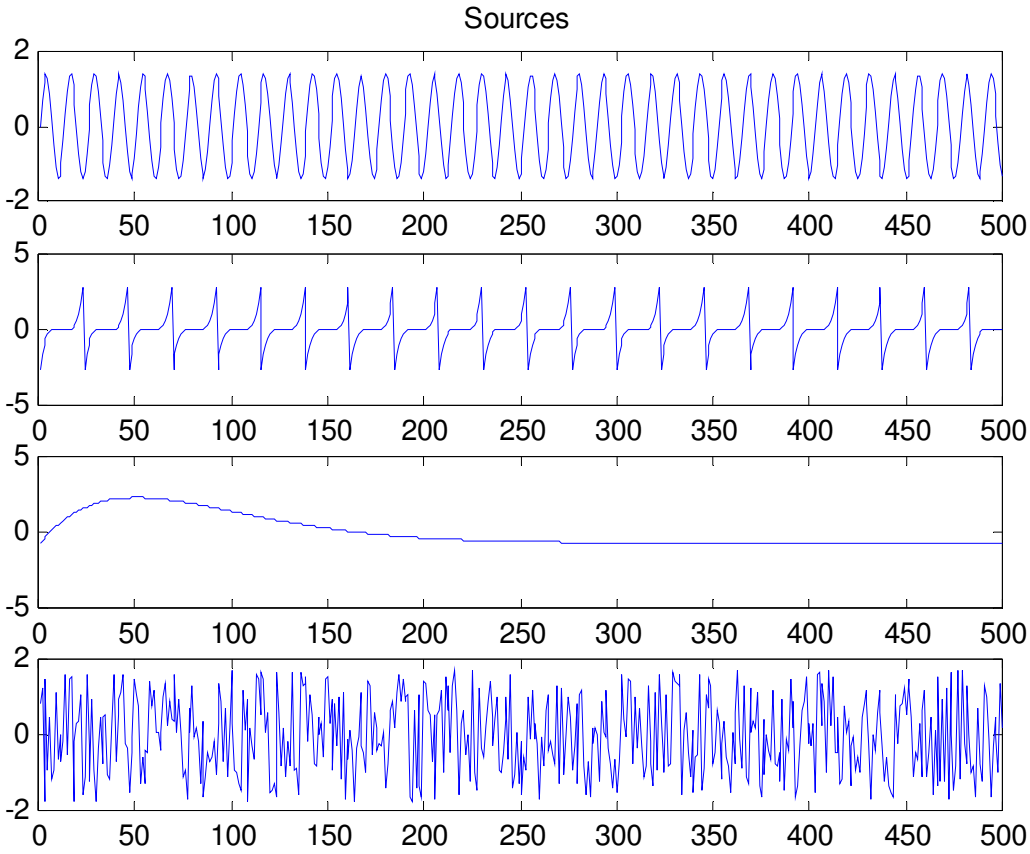

Figure 12. Original independent sources, representing the reflected signals. There are four independent sources representing reflection from a defect, reflection from a weld, reflection produced by temperature effect and random noise.

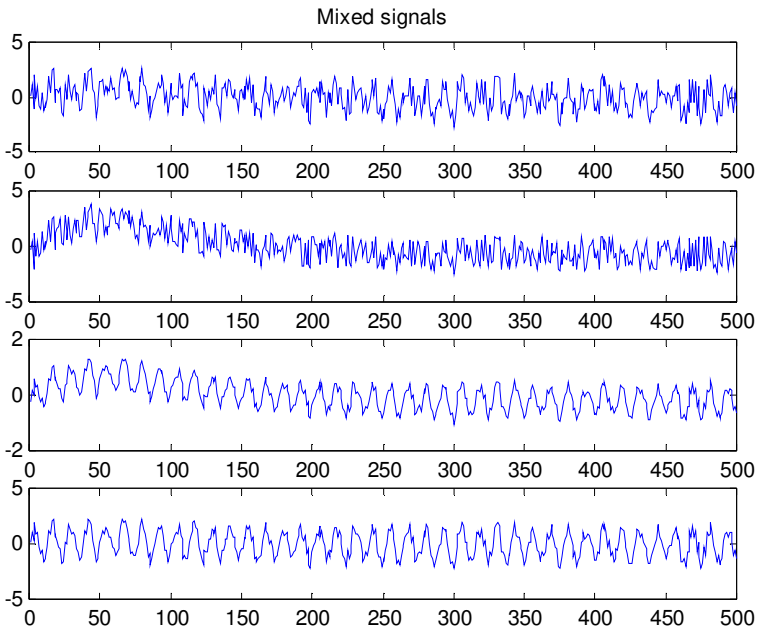

Figure 13 Mixture of the original independent sources, representing the reflected signals.

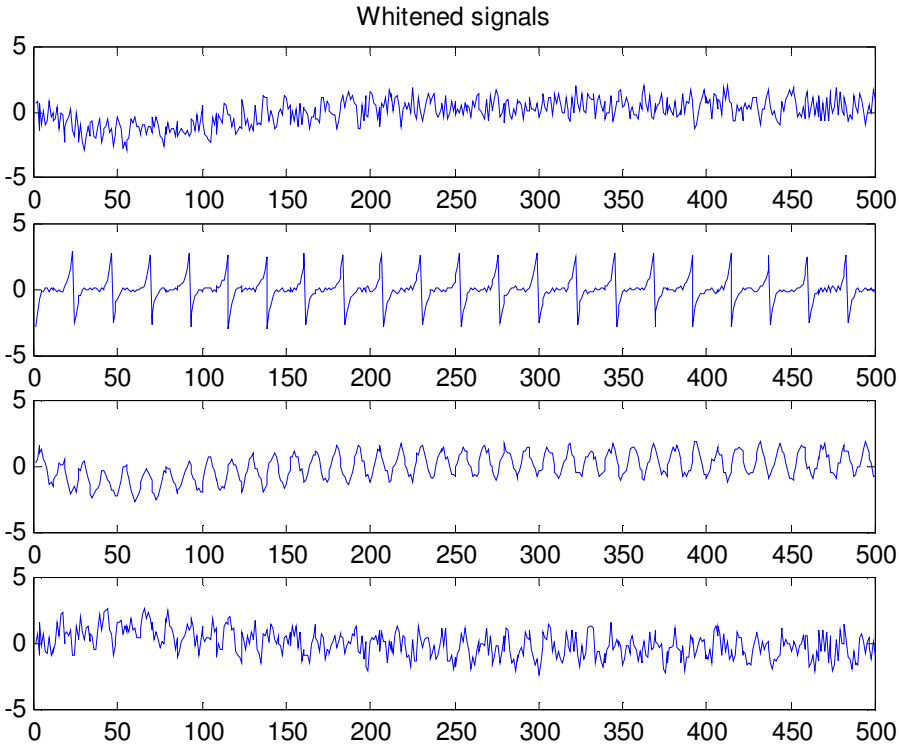

Figure 14 Results of applying PCA to the mixtures shown in previous plot.

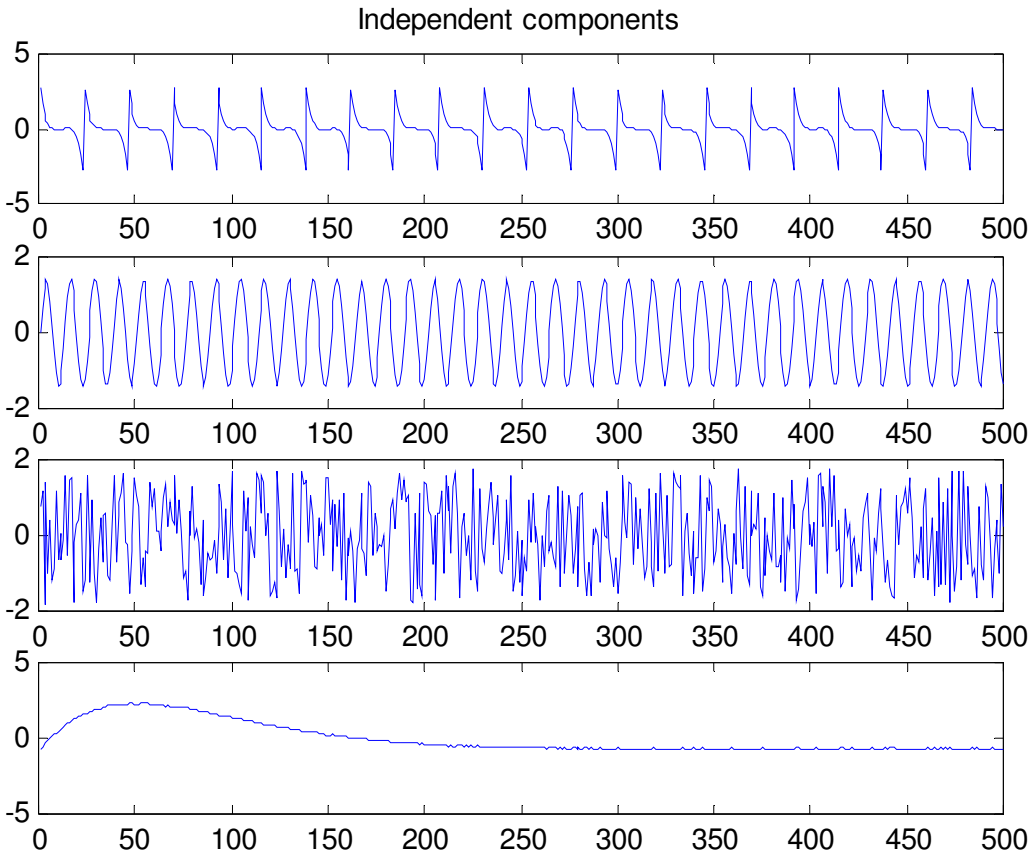

Figure 15 Results of applying FastICA to the mixture of signals.

The ICA algorithm was able to separate the simulated defect signals from coherent noise in the context of temperature changes and constant frequency content of the defect signal. In all these scenarios, the ICA algorithm was able to extract the defect signal, rejecting coherent noise.

The ICA algorithms seem to be a natural fit to separate the corrosion defect signals from coherent noise in the context of temperature changes and constant frequency content of the defect signal. Multiple GW sensors receive information from multiple sources which is combined due to interferences. This creates observed signals which align very well with fundamental ICA model. It seems that ICA has potential for filtering of GW data. However, currently available ICA algorithms have serous limitations when applied to real-world industrial data as the one utilized in this paper. Existing ICA algorithms deal with linear mixtures and require number of sources not to exceed number of sensors. While reducing the time window available to processing will reduce the number of sources in that window, in practice the number of sources is unknown. Processing axial data from the same data set will give an opportunity to work with more sources since the number of axial sensors is higher. Practically useful ICA algorithms

should be able to deal with unknown number of sources and nonlinear and convolutional mixtures. In our future work, we plan to process data from axial sensors from the same data set and study the influence of the number of sensors on the quality of separation. Also, due to invariance of ICA to ICs ordering, automatic algorithms are necessary to label ICs which can be attributed to noise, reflections from engineering features and reflections from corrosion. Since ICA does not perform dimensionality reduction, all ICs initially have to be considered useful and their ranking needs to be performed based on some other criteria than variance.

One of the benefits of having GW systems permanently installed is the ability to track defect growth by subtracting current reflections from some baseline reflections taken earlier. The results in this paper show that ICA has potential to improve SNR thus making it a tool for tracking the growth of the defects. In this future work, we plan to apply ICA to baseline subtraction to investigate opportunities for defect development monitoring. The GW system measurements were in general consistent with the measurement provided by an ultrasonic testing system in terms of locating corrosion activity on the shell. However, the GW system was unable to differentiate the defect growth during the monitoring period.

Also, it would be beneficial to study ICA's ability to deal with shadowing since it is one of the types of interference present in GW signals.

The ICA technique is also only one of several possible techniques for processing GW monitoring data. A quantitative comparison of the different techniques would indicate when each method is most appropriate. Such a comparison will also be a subject of future work.

5. HARDWARE METHODS TO EXTEND THE RANGE OF ULTRASONIC GUIDED WAVES

It has been reported in the literature that when applying UGW technology to the systems with different types of coating, the range of GWs and their propagation distance can be increased. Also, the coating can be used as additional media to propagate the wave through structural obstacles, such as elbows or bents. An especially promising aspect is that the coating is conducive to GW propagation; for example, the ones containing piezoelectric materials. In this section, we review the application of piezoelectric coating to defect detection and analyze their potential to extend the range of UGW testing. Klein et al. [71] introduced the term, "Piezoelectric paint," in 1986, in order to define composites that they had then prepared by suspending electro-ceramics and polymer in water. A conventional paint base was used and filled with lead zirconate titanate (PZT) and $PbTiO_3$ in various concentrations. This was followed by applying the paint to a surface, drying it, and then electroding and polling the painted surface to be used for sensing purposes. Further research led to improvement in the characteristic properties of the paint as well as making it more economical and easier to implement for various purposes. Several

developments led the sensor from being painted on a surface to being sprayed on one, thereby providing a uniform layer of paint on the surface.

In their work on non-destructive evaluation using piezoelectric paint sensors, Li and Zhang [72] used a suitable distributed acoustic emission sensing method for defect monitoring. They further analyzed the use of piezoelectric substances for ultrasonic signal measurements to determine the sensing capability of the piezoelectric paint. The mechanism for crack initiation detection is analyzed using a finite element simulation model calibrated using experimental data. Using finite element simulation and experimental analysis, the effect of connecting multiple sensors in an array on the output was investigated.

Based on the study, the following conclusions were reached.

- The piezoelectric paint sensor is a potential candidate for determination and monitoring of cracks in metal structures caused by fatigues.
- With increase in the number of piezoelectric sensors connected in parallel, AE signal amplitude increases.
- When the piezoelectric paint sensors are connected in parallel, capacitance of the array of sensors increases compared to a single sensor.
- Information on the detection of the AE signal is contained within the initial microseconds of the AE signals.

Li and Zhang [73] also studied the effects of piezoelectric paint sensors in acoustic emission-based monitoring of fracture, where they provide insight on the sensor's material behavior in ultrasonic sensing. A composite piezoelectric material consisting of very small piezoelectric particles randomly dispersed in a polymer matrix phase is what is called "piezoelectric paint." Fracture monitoring, or crack detection in metal, concrete, and composite structures, can be done via non-destructive evaluation methods based on acoustic emission. Effect of piezoelectric ceramic volume fraction is studied. Li and Zhang [73] have carried out an electro-mechanical analysis of piezoelectric paint sensor based on a finite element model and based on the experimental data, a simulation model was calibrated.

To summarise the feasibility of such sensors and all of the work accomplished during the period of study for this paper, the following were observed:

- Material properties of piezoelectric paint for ultrasonic sensing were modelled and analyzed. These were further used to find out the effect of the various factors that can affect the sensor's performance.
- The piezoelectric paint sensor sensitivity was significantly affected by the particle volume fraction of the PZT.

- Piezoelectric activity, comparable to that of PVDF, can be achieved by 40 to 70% PZT volume fraction piezoelectric paint.
- A 2-D coupled field finite element model was designed to validate the performance of the paint sensor and was used to further study the interaction of the subject and the sensor.
- For ultrasonic sensing in fiber-reinforced polymer (FRP) composite structures, piezoelectric paint sensors are suitable with better acoustic impedance matching.
- It is seen that judicious selection of piezoelectric ceramic and polymers, as well as the volume fraction, in order to optimise the material properties of the paint is a feasible method for AE-based fracture monitoring.

In his paper on in situ fatigue crack detection, Zhang [74] reports that the use of surface-mounted piezoelectric paint sensors and its applications are important in surface fatigue crack detection. These polymer-based piezoelectric paints can be directly applied to the surface of the subject to detect and monitor surface level cracks. Voltage is generated by the sensor when any form of mechanical strain is applied in the plane of the paint. Upon the inclusion of a special electrode design based on recent developments, a new effective method can be potentially obtained for in situ fatigue crack detection.

Detection and monitoring of fatigues can lead to a longer lifespan and better reliability of structural systems. Most of the processes in use today for fatigue detection are manual and involve high costs, intensive labor, and produced variable results. There are also NDE techniques that include eddy currents, dye penetrants, AE, magnetic particle inspection, and the like. In real-time usage, all of the NDE techniques mentioned have certain limitations due to various factors.

Continuous detection and monitoring can be achieved by advanced sensors; piezoelectric paint sensors are proposed to provide a simple yet effective technique to achieve this. The following characteristics have been noted:

- Through a series of vibration tests—including harmonic loading and free vibration tests—the dynamic strain sensing capacity of piezoelectric paint sensors was validated.
- These sensors may not provide a competitive method, such as in the case of ordinary sensing applications, when compared to conventional techniques. This is because the new sensors can’t differentiate between the two in-plain strains, thus measuring only dynamic strain.
- However, special applications like real-time monitoring of surface cracks can be performed using piezoelectric sensors.

- One shortcoming of this technique could be the generation of misleading information in case the existing cracks don't cross the sensor electrodes. This limitation can however be alleviated using complex patterned electrodes or covering a relatively smaller area.

Since the discovery of piezoelectric materials in 1980, they have gained widespread popularity in various fields. Of late, these materials have found various uses in the field of structural monitoring. Yang and Fritzen [75] studied the applications of these new piezoelectric paint sensors as spatially distributed modal sensors, one that measures a single mode while filtering the other modes of the structure. These distributed sensors are evenly and continuously distributed on the host structure, compared to conventional ones. In cases where high frequency un-modelled modes affect closed loop stability, piezoelectric sensors are useful for active control due to reduced spill-over problems. The authors, in this work, fabricated a piezoelectric paint sensor, one that is flexible and can be tailored to any shape and applied to any surface. These sensors are much easier to control based on the applications, as compared to traditional PVDFs.

Their work can be summarized by the following points.

- Piezoelectric paint when cut by hand has many inaccuracies. Cutting the edge of the modal sensor as smooth as the theoretical design is very difficult and the tip is too tiny to handle and can be damaged easily.
- Piezoelectric paint is flexible, distributable, and easy to shape.
- By placing it upside-down, the polarization profile of the sensor can be easily changed.
- Even with the existence of mode leak, the paint is still a potential composite for spatially distributed modal sensors.

Yoo et al. [76] proposed a new damage detection method based on a 2-D phased array made of piezoelectric paint to find the interaction of guided Lamb waves and various defect types. During the development of the process, they used the transverse mode of guided Lamb waves. The damage detection in isotropic thin plates is achieved by the transmission of these waves and their interaction with the boundaries and discontinuities. The group has also demonstrated the ability to detect the approaching wave-fronts' directionality, using 1-D phased sensor arrays. In order to detect the location and extent of damage on the plate, the filtering properties of various 2-D sensor arrays and signal processing techniques were employed.

The aforementioned research can thus be summarized as follows:

- Threshold setting and damage index calculation are proposed as new damage detection algorithms. These are then evaluated for the detection of simulated defects.
- Detection of simulated damages in a 2024-T3 aluminum plate is done using a newly fabricated 2-D phased sensor array with spiral configuration.
- Based on calculations, it was seen that the damage indices are directly proportional to the size of the damages.
- The limitations of the 1-D phased sensor arrays were overcome by using the proposed 2-D phased sensor arrays.
- Transient responses due to the guided Lamb waves were analyzed by applying 2-D phased array based signal processing techniques. These methods are generally used in antenna theory applications.
- Directional filtering abilities were demonstrated using sensor measurements. By eliminating any unwanted signals from the experimental signal, array responses can be improved during empirical mode decomposition.
- Noticeable wave reflections were observed from damaged regions and estimated damage locations in the resultant array responses.
- Additional information for damage location and extent was provided by the variation of the HHT amplitude with increase in damage size.

Along those lines, Yoo et al. [76,77] conducted research on SHM based on 2-D phased sensor arrays using piezoelectric-paint; hence, they also obtained similar conclusions.

Kang and Lee [78] present a piezoelectric paint sensor fabrication method. They further demonstrate its application to impact and vibration monitoring. Composed of $Pb(Nb,Ni)O_3$-$Pb(Zr,Ti)O_3$ (PNN/PZT) powder and epoxy resin, this paint is applied to an aluminum beam, while the electrode is placed on its surface using silver paste. With the application of a field voltage of 4kV/mm for about 30 minutes at room temperature, and by using the aluminium beam as the second electrode, polling of the fabricated paint is done. The vibration response of the cantilevered aluminum beam under resonance was monitored based on the output of the piezopaint sensor. Displacement strain transformation method was used in order to obtain the out-of-plane strain of the beam structure. This was compared with the strain measured by laser displacement sensors at a constant beam positon. Along those lines, the signal from the impact can be monitored by using the fabricated paint, which is sensitive to higher frequencies.

Their work on the fabrication method of the paint sensor and its applications on impact and vibration monitoring can be concluded in the following points.

- The results from the displacement strain method when compared to the out-of-plane deformation measured from the laser displacement sensors match. The position of the various defects along the length of the beam can be determined using this method.
- Impacts were made on the beam using an impact hammer. It was seen that impact forces over 10N could be captured by using the piezo paint sensor.
- PNN-PZT used in this study is a soft type piezoelectric ceramic, which makes the paint sensor high sensitive with easy polling characteristics.
- DST matrix was used to estimate the displacement by multiplying the strain data to it. Hence, maximum number of mode shapes used could be equal to the number of sensors used.
- The whole structural vibration was also calculated in addition to the one point measurements and the data was analyzed versus two measurement data.

Payo and Hale [79] designed a piezoelectric paint to be used as a strain sensor. Milled PZT powder is suspended in a lacquer to make the piezo paint. The charge generated by the sensor per electrode area relative to the strain experienced by the substrate gave the sensor's sensitivity. This value of the sensitivity was based on the hypothesis that the sum of principal strains is proportional to the charge generated. Unlike previous works where the sensitivity was calculated based on the relation between the uniaxial substrate strain and the generated charge, this work takes the biaxial strain into account also.

Based on the experimental results, the following conclusions were reached.

- From the biaxial positive bending experiments, the sensor sensitivity was calculated to be about 0.0187 (C/m2)/(m/m) with a tolerance of 0.0015.
- In the case of uniaxial bending, the sensitivity was found to be 0.0183 (C/m2)/(m/m) with a similar tolerance value.
- When subject to equal and opposite strains, the output of the piezoelectric sensor was negligible, thus confirming the hypothesis that the sum of principal strains and electrical displacements are proportional.
- Analysis of the frequency response of the strain sensor places the sensitivity of the sensor within a ±2dB range over the 5-500 Hz frequency range.

White [80] developed a piezoelectric ceramic-polymer composite for use as a thick-film strain sensor to be used for vibration monitoring. This paint can be applied onto various substances by using traditional spraying methods. The morphology of the composite and the electrodes used affected sensor properties; thus, various electrodes were tested where it was seen that the electrodes interacted with the piezo paint at

times. To study the effect of different compositions and processing conditions, SEM and light optical microscopy were performed and the material morphologies were analyzed. Heat treatment is done to anneal out the defects produced during the milling process and was followed by X-ray analysis and particle size analysis to characterize any changes during the process. X-ray diffractometry was done to study the effect of polling. The following inferences were made based on this study:

- A potential coating system was developed with piezoelectric properties for use as a sensor for vibration monitoring in structures.
- The piezo paint sensors were found to have a very dynamic range with a bandwidth of 1-2 kHz and a microstrain range of 40-4000.
- The piezoelectric coefficient was found to be 20 pC/N approximately for d_{31}.
- The field trial results were successful showing that the sensors are resistant to outdoor exposure.
- All the trials and measurements were performed within the abovementioned bandwidth and not outside. Expected bandwidth values are significantly broader.

In his work, Hale [81] describes the development of thick-film sensors made of piezo paint for shock and vibration monitoring in structures. Characterization of properties of the thick-film sensor is done to show the dynamic range and bandwidth necessary for structural monitoring and robustness of the sensor. The new sensor, even if not ideal, is an improvement over the earlier type such that it can be sprayed on instead of scraping on with a blade. Piezoelectric sensors are conventionally fabricated by screen printing inks on a substrate. Using paints instead of inks makes it advantageous as it is suitable for uneven and curved surfaces as well, while also being able to be cured at room temperature. Thus, with the advantages of thick-film sensors, these piezo paint sensors can be used on large complex surfaces, as well as temperature sensitive materials.

Based on the study and field work, the following conclusions were drawn:

- The newly developed paint allows a greater concentration of piezoelectric ceramic powder, is easy to spray on surfaces and is curable at room temperatures.
- Electrodes and wire connections for signal transmission can be made out of compatible materials.
- Reliable sensors can be made in bulk commercially based on established spraying and polling conditions.
- The dynamic range and bandwidth were found to be in a range suitable for structural monitoring of shocks and vibrations.

- A field test was performed by placing a sensor on a footbridge and monitoring it over a period of three years. Not much deterioration exists other than a slight loss in sensitivity over the years.

Zhang [82] discusses crack monitoring and damage detection in complex structures by using piezoelectric paint sensors. Real-time continuous on-line SHM requires the use of advanced sensors. Traditionally available ceramics are not ideal for use in such applications, thus leading to the development of polymer-based piezo paint sensor. By constantly measuring the output voltage signals from the piezo sensors, one can monitor the dynamic responses of the host subject. These sensors hold great potential since their properties can be easily calibrated, they are economical, easy to implement, and can be used on a multitude of surfaces. The various characteristics of this particular sensor include the ability to measure dynamic strain and not static load; being used as a surface-mounted sensor and the paint can be applied on rough and curved surfaces; it is self-powered and needs no external excitation; and it can be used to measure strain in one direction from the output voltage value. The output of the sensor is AC voltage, which can be given into any data acquisition system, thus eliminating the need for synchronization. Summarizing the work presented in his paper, we can come to the following conclusions:

- Through a series of preliminary studies, a new method of piezoelectric paint application on to surfaces was developed.
- Vibration tests, impact hammer tests, and harmonic loading tests were performed and the damage index was calculated.
- As an active sensor, the piezoelectric paint sensor can be used to monitor in real-time the dynamic one-directional strains, without the application of any external voltage.
- Using multi-electrode combinations along with the piezo sensor, a novel technique for surface crack detection was proposed and experimentally validated.

In order to determine the effects posed to piezoelectric paint sensors when exposed to environmental conditions, such as rain, Raptis et al. [83] performed an experiment utilizing PZT particles in an acrylic lacquer. Samples coated with piezoelectric paint were submerged in both water and potassium iodide solutions for different periods of time and then tested in terms of the potential sensitivity of the piezoelectric paint. They discovered that after a drying period, which was dependent on the time submerged, not only did the piezoelectric paint sensors recover to their original functioning state, they possessed an initial increase in sensitivity especially when submerged in the potassium iodide solution. While the cause of this phenomenon of enhanced sensitivity is not yet understood, it could lead to two different outcomes:

- Either these measurements will fail to be reproduced.

- Enhanced sensitivity of piezoelectric paint will be obtained with further understanding and control.

In a different study also aimed at determining the effects of weather on the capabilities and longevity of piezoelectric paint, Hale and Lahtinen [84] performed trials on two established bridges over a period of two and six years utilizing an acrylic-based and epoxy-based piezoelectric paint, respectively. The results of these trials concluded that:

- Aging of piezoelectric paint is relatively unaltered when exposed to a wide range of environmental conditions, such as sunlight, rain, snow, and frost.
- Piezoelectric paint sensitivity drops within the first few months, but soon levels out to a stable and constant state.
- After the test period, the piezoelectric paint was determined to be nowhere near the end of its life-cycle despite exposure to harsh environmental conditions.

A large issue of utilizing piezoelectric paint is the fact that no standards exist in terms of fabrication. In an attempt to identify certain properties of piezoelectric paint such as microstructure, tensile strength, and sensitivity for the purpose of creating a standard fabrication procedure, Yang and Fritzen [85,86] performed a range of tests on samples of piezoelectric paint using the tape-casting method. While other methods of utilizing piezoelectric paint exist, such as spraying on or screen-printing, the tape-casting method seems to be superior as it can be used in a wider range of applications. The spraying method can only be used in situations where the material to which the paint is applied is conductive, while the screen-printing method only produces thick films over a specific area. In terms of microstructure, it was determined that the maximum weight percentage is 60%, with 50% being ideal, before severe air voids become present. These voids reduce the strength of adhesion between the piezoelectric particles and can lead to dielectric breakdown during polling. Tensile strength tests confirmed that the piezoelectric paint produced by the tape casting method can be applied to a wide range of applications. Upon analysis of the sensitivity of the piezoelectric paint, it was determined that the piezoelectric charge constant was close to a published calculation that concludes the overall effectiveness of the paint.

In several studies to determine the effects of film thickness, cure temperature, polling field, and volume fraction of PZT on the sensitivity of piezoelectric paint to be utilized as a vibration sensor or an AE sensor, Egusa and Iwasawa [87,88,89] made the following conclusions:

- Sensitivity was nearly identical for cure temperatures of 25°C and 150°C for a film thickness of less than 30μm.

- As film thickness increases above 30μm, increases in sensitivity are greater at a cure temperature of 25°C versus 150°C.
- Sensitivity increases with an increase in polling field and film thickness but is limited by eventual electrical breakdown at high levels of polling field.
- Sensitivity increases with an increase in volume fraction from 30 to 53%.

In an attempt to determine the effectiveness at utilizing a piezoelectric film AE sensor to monitor fatigue crack growth in welded tubular structures, Zhang et al. [90] discovered the following relationships between the frequency of AE signals and source mechanism:

- AE signals induced by friction of the fatigue crack surface were of relatively low frequency.
- AE signals induced by fatigue crack propagation were of relatively high frequency.
- This difference in induced frequency can be used to determine whether AE signals are due to friction between the crack surfaces or due to crack propagation, which therefore aids in monitoring the lifespan of the structure.

Yoo et al. [91] utilized several 2-D phased sensor arrays each composed of 25 piezoelectric paint sensors on an aluminum plate. The two arrays, cruciform and spiral, were specifically designed to allow not only the severity of damage to be determined, but also the damaged regions within the array based on the induced signal.

In order to determine the effectiveness of piezoelectric paint as a dynamic strain measurement sensor, Zhang [92] performed both harmonic excitation and impact hammer tests on an aluminum beam coated with a piezoelectric paint composed of PZT-5A. Analysis of the impact hammer tests show that the piezoelectric paint sensor's output is proportional to the force of the impact and was shown to have high repeatability with similar forces. Analysis of the harmonic excitation tests show that the piezoelectric paint sensor's output clearly matches that of the range of excitation frequencies used. The tests concluded that piezoelectric paint sensors are very effective at monitoring dynamic strain on a system.

Li and Zheng [93] conducted extensive research on a micromechanical constitutive model for flexible piezoelectric paint based on percolation property. They came up with the following conclusions:

- Piezoelectric paint was quite advantageous when used as smart sensing materials. This includes the flexible mechanical properties and its conformability to easily get surfaced with complicated geometries.

- Piezoelectric paints that possess a ceramic volume fraction in the range of 35% to 65% result in formation of 1-3 connectivity, which further leads to higher piezoelectric activity in the composite material.
- Some of the special features like mixed connectivity and air void content have been addressed by means of a micromechanics constitutive model for piezoelectric paints. This is done by implementing the universal scaling law of percolation theory.
- The good agreement between the predicted electromagnetic characteristics of the piezoelectric composites and the experimental data obtained provides solid verification of the effectiveness of the percolation based mixed connectivity model (PMCM).

We can conclude that piezoelectric paint is a potential material that can be used to monitor structural shocks and vibrations. It can also be used to extend the range of GW techniques through coating. Characterization of the piezoelectric paint suggests that it is much more economical and easier to implement when compared with traditional sensors. The piezo paint material possesses a dynamic range and has a much higher bandwidth. With respect to conventional film sensors, piezo paint sensors have various advantages, such as greater area coverage, applicability on rough and complex surfaces, independent of external excitation voltage, and absence of binding adhesive between the host and the sensor. The dynamic strain of a structure can be monitored by real-time measurement of the output AC voltage of the sensor. It also finds applications in online damage monitoring and surface crack detection, and has been shown to resist environmental conditions when used over a long period.

6. REFERENCES

1. Area monitoring using ultrasonic guided wave. [Online]. Available at: http://www.imperial.ac.uk/non-destructive-evaluation/research/inspection-and-monitoring/area-monitoring-using-ultrasonic-guided-wave/.
2. Alleyne, D., Vogt, T., and Pavlakovic, B. (2016). Monitoring corrosion with guided waves. Electric Power Research Institute Workshop for Structural Health Monitoring of Passive Components, EPRI Charlotte Office, April 13–14.
3. Lowe, M.J.S., Alleyne, D.N., and Cawley, P. (1998). Defect detection in pipes using guided waves. *Ultrasonics*, 36(1–5), 147–154.
4. Li, J. (2005). On circumferential disposition of pipe defects by long-range ultrasonic guided waves. *J. Pressure Vessel Technol.*, 127(4), 530–537.
5. Zhu, W. (2002). An FEM simulation for guided elastic wave generation and reflection in hollow cylinders with corrosion defects. *J. Pressure Vessel Technol.*, 124(1), 108–117.
6. Demma, A. (2004). The reflection of guided waves from notches in pipes: A guide for interpreting corrosion measurements. *NDT and E Int.*, 37(3), 167–180.
7. Kharrat, M., Zhou, W., Bareille, O., and Ichchou, M. (2011). Defect detection in pipes by torsional guided-waves: A tool of recognition and decision-making for the inspection of pipelines. In *EURODYN 2011, Proceedings of the 8th International Conference on Structural Dynamics.* Leuven, Belgium, 4–6 July. De Roeck, G., Degrande, G., Lombaert, G., and Müller, G. (eds.).
8. Zheng, M.-F., Lu, C., Chen, G.-Z., and Men, P. (2011). Modeling three-dimensional ultrasonic guided wave propagation and scattering in circular cylindrical structures using finite element approach. *Physics Procedia*, 22, 112–118.
9. ANSYS Mechanical APDL Theory Reference. ANSYS Rel. 14.5—Canonsburg: ANSYS Inc., (2012).
10. Cau, F., Fanni, A., Montisci, A., Testoni, P., and Usai, M. (2006). A signal-processing tool for non-destructive testing of inaccessible pipes. *Eng. Appl. Artif. Intell.*, 19(7), 753–760.
11. Landau, L.D. and Lifshitz, E.M. *Theory of Elasticity*, volume 7 of *Course of Theoretical Physics*. Pergamon Press, New York, 1959.
12. Acciani, G., Brunetti, G., Fornarelli, G., and Giaquinto, A. (2010). Angular and axial evaluation of superficial defects on non-accessible pipes by wavelet transform and neural network-based classification. *Ultrasonics*, 50(1), 13–25.
13. Lee, H., Yang, J., and Sohn, H. (2012). Baseline-free pipeline monitoring using optical fiber guided laser ultrasonics. *Struct. Health Monit.*, 11(6), 684–695.
14. Ahmad, R., and Kundu, T. (2011). Cylindrical guided wave signals for underground pipe inspection using different continuous wavelet mother functions. *J. Civil Eng. Arch.*, 5(12), 1103–1110.
15. Lee, C., and Park, S. (2015). Damage visualization of pipeline structures using laser-induced ultrasonic waves. *Struct. Health Monit.,* 14(5), 475–488.
16. Mu, J., Zhang, L., and Rose, J. L. (2007). Defect circumferential sizing by using long range ultrasonic guided wave focusing techniques in pipe. *Nondestruct. Test. Eva.*, 22(4), 239–253.
17. Ni, J., Zhou, S., Zhang, P., and Li, Y. (2016). Effect of pipe bend configuration on guided waves-based defects detection: An experimental study. *J. Pressure Vessel Technol.*, 138(2), 021203–021203-9.

18. Wang, X., Peter, W. T., and Dordjevich, A. (2011). Evaluation of pipeline defect's characteristic axial length via model-based parameter estimation in ultrasonic guided wave-based inspection. *Meas. Sci. Technol.*, 22(2), 025701.

19. Cobb, A. C., and Fisher, J. L. (2016). Flaw depth sizing using guided waves. In *42nd Annual Review of Progress in Quantitative Nondestructive Evaluation: Incorporating the 6th European-American Workshop on Reliability of NDE.* AIP Publishing, Minneapolis, MN, USA.

20. Otero, R., Moreno, E., and Meza, B. (2011). Generation of focused ultrasonic guided waves for nondestructive testing of structures. In *5th Pan American Conference for NDT.* NDT.net., Cancun, Mexico.

21. Cheng, J.-W., Yang, S.-K., and Chiu, S.-M. (2007). The use of guided waves for detecting discontinuities in fluid-filled pipes. *Mater. Eval.*, 65(11), 1129–1134.

22. Gori, M., Giamboni, S., D'Alessio, E., Ghia, S., Cernuschi, F., and Piana, G. M. (1996). Guided waves by EMAT transducers for rapid defect location on heat exchanger and boiler tubes. *Ultrasonics*, 34(2), 311–314.

23. Lu, B., Upadhyaya, B. R., and Perez, R. B. (2005). Structural integrity monitoring of steam generator tubing using transient acoustic signal analysis. *IEEE T. Nucl. Sci.*, 52(1), 484–493.

24. Leinov, E., Lowe, M. J. S., and Cawley, P. (2015). Investigation of guided wave propagation and attenuation in pipe buried in sand. *J. Sound Vib.*, 347, 96–114.

25. Leinov, E., Lowe, M. J. S., and Cawley, P. (2016). Ultrasonic isolation of buried pipes. *J. Sound Vib.*, 363, 225-239.

26. Ahmad, R. (2005). *Guided Wave Technique to Detect Defects in Pipes Using Wavelet Analysis.* (Doctoral Dissertation), University of Arizona, Arizona, USA.

27. Lowe, M. J. S., and Cawley, P. (2006). *Long range guided wave inspection usage–Current commercial capabilities and research directions.* Department of Mechanical Engineering, Imperial College London, London.

28. Cawley, P. (2002). Practical long range guided wave inspection – Applications to pipes and rails. In *NDE2002: National Seminar of Indian Society for Non-Destructive Testing*. NDT.net., Chennai, India.

29. Rose, J. L. (2009). Successes and challenges in ultrasonic guided waves for NDT and SHM. In *NDE2009: National Seminar & Exhibition on Non-Destructive Evaluation*. NDT.net., Tiruchirappalli, India.

30. Mokhles, M., Ghavipanjeh, C., and Tamimi, A. (2013). The use of ultrasonic guided waves for extended pipeline qualification prediction. In *SINCE2013: Singapore International NDT Conference & Exhibition*. NDT.net., Marina Bay Sands, Singapore.

31. Na, W.-B., and Kundu, T. (2002). Underwater pipeline inspection using guided waves. *J. Pressure Vessel Technol.*, 124(2), 196–200.

32. Rizzo, P. (2010). Water and wastewater pipe nondestructive evaluation and health monitoring: A review. *Advances in Civil Engineering*, 2010.

33. Vasiljevic, M., Kundu, T., Grill, W., and Twerdowski, E. (2008). Pipe wall damage detection by electromagnetic acoustic transducer generated guided waves in absence of defect signals. *J. Acoust. Soc. Am.*, 123(5), 2591–2597.

34. Ahmad, R., and Kundu, T. (2012). Structural health monitoring of steel pipes under different boundary conditions and choice of signal processing techniques. *Advances in Civil Engineering*, 2012.

35. Demma, A., Cawley, P., Lowe, M., Roosenbrand, A.G., & Pavlakovic, B. (2004). The reflection of guided waves from notches in pipes: A guide for interpreting corrosion measurements. *NDT and E Int.*, 37(3), 167–180.

36. Sun, P., Wu, X., Li, J., & Wang, Y. (2015). An EMAT for inspecting heat exchanger tubes of stainless steel using longitudinal guided waves based on non-uniform static magnetic fields. *Insight-Non-Destructive Testing and Condition Monitoring*, 57(4), 221–229.

37. Sinding, K., Searfass, C., Malarich, N., Reinhardt, B., and Tittmann, B. R. (2013). High temperature ultrasonic transducers for the generation of guided waves for non-destructive evaluation of pipes. In *QNDE2013-ICBM2013: 40th Annual Review of Progress in Quantitative Nondestructive Evaluation: Incorporating the 10th International Conference on Barkhausen Noise and Micromagnetic Testing*. AIP Publishing, Baltimore, MD, USA.

38. Bezdek, M., Joseph, K., Guers, M., and Tittmann, B. R. (2008). Structural health monitoring and nondestructive evaluation of double wall structures. In *SPIE6935: Health Monitoring of Structural and Biological Systems*. San Diego, CA, USA: International Society for Optics and Photonics.

39. Kwun, H., Crane, J. F., Kim, S. Y., Parvin, A. J., and Light, G. M. (2005). A torsional mode guided wave probe for long range, in bore testing of heat exchanger tubing. *Mater. Eval.*, 63(4), 430–433.

40. Cheong, Y.-M., Lee, D.-H., Kim, S.-S., and Jung, H.-K. (2004). Analysis of the circumferential guided wave for axial crack detection in a feeder pipe. *Key Eng. Mater.*, 270–273, 422–427.

41. Puchot, A. (2013). Continued monitoring and analysis of MSS data collected on the Braidwood heat exchanger shell 13A, Final Report SwRI Project No. 18.18166.02. March 7.

42. Joliffe, I. T. (1986). Principal Component Analysis, Springer-Verlag, New York, NY, USA.

43. Hyvarinen, A. (1999a). Fast and robust fixed-point algorithms for independent component analysis. *IEEE T. Neural Networks*, 10(3), 626–634.

44. Hyvarinen, A. (1999b). Survey on independent component analysis. *Neural Computing Surveys*, 2, 94–128.

45. Hyvarinen, A., Karhunen, J., and Oja, E. (2001). Independent Component Analysis. John Wiley & Sons, New York, NY, USA.

46. Huber, P. J. (1985). Projection pursuit. *Ann. Stat.,* 13(2), 435–475.

47. Burel, G. (1992). A nonlinear neural algorithm. *Neural Networks*, 5, 937–947.

48. Lewicki, M., and Sejnowski, T. J. (2000). Learning over complete representations. *Neural Comput.*, 12(2), 337–365.

49. Nadal, J. P., and Parga, N. (1994). Non-linear neurons in the low noise limit: A factorial code maximizes information transfer. *Network*, 5, 565–581.

50. Matsuoka, K., Ohya, M., and Kawamoto, M. (1995). A neural net for blind separation of nonstationary signals. *Neural Networks*, 8(3), 411–419.

51. Molgedey, L., and Schuster, H. G. (1994). Separation of a mixture of independent signals using time delayed correlations. *Phys. Rev. Lett.*, 72, 3634–3636.

52. Deco, G., and Obradovic, D. (1996). An Information-Theoretic Approach to Neural Computing. Springer-Verlag, New York, NY, USA.

53. Shannon, C. E. (1948). A mathematical theory of communication. *Bell Sys. Tech. J.*, 27, 379–423.

54. Girolami, M. (1999). Self-Organising Neural Networks, Independent Component Analysis, and Blind Source Separation. Springer-Verlag, New York, NY, USA.

55. Lowe, M. and Cawley, P. (2006). Long range guided wave inspection usage - Current commercial capabilities and research directions. Department of Mechanical Engineering, Imperial College London. [Online]. Available at: http://www3.imperial.ac.uk/pls/portallive/docs/1/55745699.PDF.

56. Cawley, P., Cegla, F., and Galvagni, A. (2012). Guided waves for NDT and permanently-installed monitoring. *Insight*, 54, 594–601.

57. Guided Ultrasonics, Ltd. [Online]. Available at: http://www.guided-ultrasonics.com.

58. Plant Integrity, Ltd. (2015). Teletest focus. [Online]. Available at: http://www.plantintegrity.com/teletest/teletest-focus/.

59. Guided Wave Analysis, LLC. [Online]. Available at: http://www.gwanalysis.com.

60. Carandente, R., and Cawley, P. (2010). The scattering of the fundamental torsional mode from axi-symmetric defects with varying depth profiles in pipes. *J. Acoust. Soc. Amer.*, 127, 3440–3448.

61. Lovstad, A., and Cawley, P. (2011). The reflection of the fundamental torsional guided wave from multiple circular holes in pipes. *NDT and E Int.*, 44, 553–562.

62. Galvagni, A., and Cawley, P. (2011). The reflection of guided waves from simple supports in pipes. *J. Acoust. Soc. Amer.*, 129, 1869–1880.

63. Thompson, D., and Chimenti, D. (Eds.). (2003). *Practical Long Range Guided Wave Inspection-Managing Complexity*, 657. American Institute of Physics. College Park, MD, USA.

64. Croxford, A., Wilcox, P., and Drinkwater, B. (2007). Strategies for guided-wave structural health monitoring. *Proc. Royal Soc. A*, 463, 2961–2981.

65. Lu, Y., and Michaels, J. (2005). A methodology for structural health monitoring with diffuse ultrasonic waves. *Ultrasonics*, 43, 717–731.

66. Liu, C., Harley, J., Berges, M., Greve, D., and Oppenheim, I. (2015). Robust ultrasonic damage detection under complex environmental conditions using singular value decomposition. *Ultrasonics*, 58, 75–86.

67. Park, H., Sohn, H., Law, K., and Farrar, C. (2009). Time reversal active sensing for health monitoring of a composite plate. *J. Sound Vibration*, 302, pp. 50–66.

68. Lu, Y., and Michaels, J. (2009). Feature extraction and sensor fusion for ultrasonic structural health monitoring under changing environmental conditions. *IEEE Sensors J.*, 9(11), 1462–1471.

69. Liu, C., et al. (2013). Singular value decomposition for novelty detection in ultrasonic pipe monitoring. In *Proc. Sensors Smart Structures Technol. Civil, Mech., Aerosp. Syst.* Lynch, J. P., Yun, C.-B., and Wang, K.-W. (Eds.). vol. 8692, San Diego, CA, USA.

70. Galvagni, A., and Cawley, P. (2014). Reliable identification of damage growth using guided wave SHM systems. In: *EWSHM2014: 7th European Workshop on Structural Health Monitoring and 2nd European Conference of the Prognostics and Health Management (PHM) Society*. National Institute for Research in Computer Science and Control. Nantes, France.

71. Klein, K. A., Safari, R. E., Newnham, R. E., and Runt, J. (1986). Composite piezoelectric paints. In: *ISAF86: 6th IEEE International Symposium on Applications of Ferroelectrics*. Institute of Electrical and Electronics Engineers. Bethlehem, PA, USA.

72. Li, X., and Zhang, Y. (2007). Piezoelectric paint sensor for ultrasonic NDE. In: *SPIE6529: Sensors and Smart Structures Technologies for Civil, Mechanical, and Aerospace Systems*. International Society for Optics and Photonics. San Diego, CA, USA.

73. Li, X., and Zhang, Y. (2008). Analytical study of piezoelectric paint sensor for acoustic emission-based fracture monitoring. *Fatigue Fract. Eng. M.*, 31(8), 684–694.

74. Zhang, Y. (2006). In situ fatigue crack detection using piezoelectric paint sensor. *J. Intel. Mat. Syst. Str.*, 17(10), 843–852.

75. Yang, C., and Fritzen, C.-P. (2011). Piezoelectric paint as spatially distributed modal sensors. In: *8th International Workshop on Structural Health Monitoring*. DEStech Publications Inc. Stanford, CA, USA.

76. Yoo, B., Pines, D. J., Purekar, A. S., and Zhang, Y. (2010). Piezoelectric paint based 2-D sensor array for detecting damage in aluminum plate. In: *51st AIAA/ASME/ASCE/AHS/ASC Structures, Structural Dynamics, and Materials Conference*. American Institute of Aeronautics and Astronautics Inc. Orlando, FL, USA.

77. Yoo, B., Purekar, A. S., Zhang, Y., and Pines, D. J. (2010). Piezoelectric-paint-based two-dimensional phased sensor arrays for structural health monitoring of thin panels. *Smart Mater. Struct.*, 19(7), 1–17.

78. Kang, L.-H., and Lee, J.-R. (2014). Piezoelectric paint sensor for impact and vibration monitoring. In: *EWSHM2014: 7th European Workshop on Structural Health Monitoring and 2nd European Conference of the Prognostics and Health Management (PHM) Society*. National Institute for Research in Computer Science and Control. Nantes, France.

79. Payo, I., and Hale, J. M. (2010). A piezoelectric paint thick-film strain sensor for vibration monitoring purposes. In: *ISMA2010: 24th International Conference on Noise and Vibration Engineering and 3rd International Conference on Uncertainty in Structural Dynamics*. University of Leuven. Leuven, Belgium.

80. White, J. R., De Poumeyrol, B., Hale, J. M., and Stephenson, R. (2004). Piezoelectric paint: Ceramic-polymer composites for vibration sensors. *J. Mater. Sci.*, 39(9), 3105–3114.

81. Hale, J. M. (2004). Piezoelectric paint: Thick-film sensors for structural monitoring of shock and vibration. In: *ESDA2004: 7th Biennial Conference on Engineering Systems Design and Analysis*. American Society of Mechanical Engineers. Manchester, UK.

82. Zhang, Y. (2005). Piezoelectric paint sensor for real-time structural health monitoring. In: *SPIE5765: Smart Structures and Materials 2005: Sensors and Smart Structures Technologies for Civil, Mechanical, and Aerospace Systems*. International Society for Optics and Photonics. San Diego, CA, USA.

83. Raptis, P. N., Stephenson, R., Hale, J. M., and White, J. R. (2004). Effect of exposure of piezoelectric paint to water and salt solution. *J. Mater. Sci.*, 39(19), 6079–6081.

84. Hale, J. M., and Lahtinen, R. (2007). Piezoelectric paint: Effects of harsh weathering on aging. *Plast. Rubber Compos.*, 36(9), 419–422.

85. Yang, C., and Fritzen, C.-P. (2012a). Piezoelectric paint: Characterization for further applications. *Smart Mater. Struct.*, 21(4), 045017.

86. Yang, C., and Fritzen, C.-P. (2012b). Characterization of piezoelectric paint and its refinement for structural health monitoring applications. In: *SPIE8409: 3rd International Conference on Smart Materials and Nanotechnology in Engineering*. International Society for Optics and Photonics. Shenzhen, China.

87. Egusa, S., and Iwasawa, N. (1998). Piezoelectric paints as one approach to smart structural materials with health-monitoring capabilities. *Smart Mater. Struct.*, 7(4), 438–445.

88. Egusa, S., and Iwasawa, N. (1996). Application of piezoelectric paints to damage detection in structural materials. *J. Reinf. Plast. Comp.*, 15(8), 806–817.

89. Egusa, S., and Iwasawa, N. (1994). Preparation of piezoelectric paints and application as vibration modal sensors. *J. Intel. Mat. Syst. Str.*, 5(1), 140–144.

90. Zhang, Y., Zhou, C., and Tong, L. W. (2014). Fatigue crack growth monitoring of welded tubular structures using piezoelectric film acoustic emission sensor. In: *IABMAS2014: 7th International Conference of Bridge Maintenance, Safety and Management*. Taylor and Francis – Balkema. Shanghai, China.

91. Yoo, B., Pines, D. J., and Purekar, A. S. (2009). 2-D directional phased array using piezoelectric paint to detect damages in isotropic plates. In: *SMASIS2009: ASME 2009 Conference on Smart Materials, Adaptive Structures and Intelligent Systems*. American Society of Mechanical Engineers. Oxnard, CA, USA.

92. Zhang, Y. (2003). Dynamic strain measurement using piezoelectric paint. In: *IWSHM2003: 4th International Workshop on Structural Health Monitoring: From Diagnostics and Prognostics to Structural Health Management*. DEStech Publications. Stanford, CA, USA.

93. Li, X., and Zhang, Y. (2008). A percolation based micromechanical constitutive model for flexible piezoelectric paint. In: *SMASIS2008: ASME 2008 Conference on Smart Materials, Adaptive Structures and Intelligent Systems*. American Society of Mechanical Engineers. Ellicott City, MD, USA.